Supplemental Finfish Survey Targeting Mid-Atlantic Migratory Species

2006 Reference Document

Sarah E. King
Eric N. Powell

Haskin Shellfish Research Laboratory
Rutgers University
6959 Miller Ave.
Port Norris, NJ 08349

Funded by the
MAFMC Research Set-Aside Program
to the
National Fisheries Institute – Scientific Monitoring Committee
and
Haskin Shellfish Research Laboratory – Rutgers, The State University of New Jersey

Table of Contents

Introduction and Rationale

Improving estimates of stock abundance by improving the underlying databases that support these estimates is a constant goal in fisheries management and stock assessment biology. One target of survey augmentation is the development of ways to better evaluate how seasonal migration of fish in the Mid-Atlantic influences stock abundance estimates. One important characteristic of many commercially and recreationally important species is the north-south and onshore-offshore migration that occurs in late fall and the following spring (Shephard and Terceiro, 1994; Murawski, 1993). Species such as *Loligo* squid, scup, spiny dogfish, and summer flounder move inshore and upcoast in the late spring as the water warms and then move downcoast and offshore in the late fall as the water cools (Jensen, 1965; NEFSC, 1998; NOAA, 1999; NRDC, 2001).

The spatial-temporal dynamics in the movement of these species is predictable in general form, but less so in specific timing and spatial extent. Fish move offshore at different times in different years and farther downcoast in some years than in others. These dynamics in the distribution of commercially and recreationally important Mid-Atlantic species presents a challenge in stock assessment. NMFS-NEFSC* conducts three surveys annually, one in early fall (September-October), one in winter (February), and one in early spring (March-April) (e.g., NEFSC, 1999). The winter and spring surveys take place during the time when these fish are moving offshore and downcoast. Consequently, survey catches will be influenced by the status of the migratory event at the time of the survey.

The initial impetus for the Supplemental Finfish Survey was to provide additional information on the migratory status of a variety of recreationally and commercially important Mid-Atlantic species. As the survey design was developed, however, three additional goals were addressed. The second was the determination of the extent to which some fish stocks extend into deep water beyond the region of the federal surveys. The NMFS-NEFSC bottom trawl surveys have a stratified random sampling design. Due to the wide area that must be sampled and constraints on total survey time, many of the offshore strata are sampled at a minimum sampling intensity (2-3 samples per stratum). Species such as monkfish, winter flounder, spiny dogfish, and *Loligo* and *Illex* squid often are abundant beyond the 175-200 fm limit of the federal surveys. As the fish move offshore, they concentrate in the offshore strata near the edge of the survey domain in a relatively small region and in a temporally unstable manner. The scale of species patchiness or clustering in time and space, in part determined by the dynamics of migration, may result in insufficient sampling density in some strata during some years. In a recent *Loligo* stock assessment (NEFSC, 2002), for example, the model used for

* National Marine Fisheries Service-Northeast Fisheries Science Center

catchability explicitly included a variable describing the unsurveyed component of the stock that is presumed to exist during the time of the spring survey as squid migrate out of the surveyed area.

A third goal, the importance of which has increased as the survey progressed, is the detailed depiction of cross-shelf distributional patterns of species. These data have proven valuable in addressing questions concerning the overlap of target and discard species because the transect format provides a relatively unbiased rendering of these distributional patterns. The recent interest in the relationship between scup and *Loligo* squid is an example (Powell et al., 2004). Thus, the survey is designed to provide data on cross-shelf distributional patterns at a spatial resolution greater than the federal stock surveys. Underwood (1978) provides a theoretical treatment of transect sampling for species distributions.

A final goal is the testing of an adaptive sampling strategy detailed in a later section. Adaptive sampling is an approach predicated on the maximization of desired information with minimal sampling. In the case of the Supplemental Finfish Survey, the desired information is the detailed documentation of the cross-shelf distribution of species on the outer shelf and improving of the estimate of biomass and abundance across this depth gradient. Among other important outcomes of this sampling strategy is an evaluation of the importance of sample density across the depth gradient and an examination of the value of adaptive sampling to increase accuracy in survey biomass and abundance estimates.

2006 Survey Design and Implementation Protocols

To develop a survey that tracks the seasonal movements of selected fish species, offshore and downcoast in the fall coincident with declining temperatures and upcoast and onshore as the water warms in the spring, the survey design includes spatial and temporal components. To extend this supplemental survey beyond the domain of present-day NMFS-NEFSC surveys, sampling intensity is increased between 150 and 250 fm. Finally, to describe the cross-shelf distribution of species, the sampling program includes fixed, depth-structured samples plus adaptive stations to enhance the resolution of species' distributions.

The present survey design is a modification of an original survey design developed in 2002 brought about by funding restrictions that limited the total number of transects sampled and changes in sampling protocol to improve survey quality. The original survey design and the history of survey modifications will be detailed in a later section.

Organization of Stations in Time and Space

The Supplemental Finfish Survey carries out sampling programs four times

during the year, in November, January, March, and May. The November to May emphasis brackets the time period of migration for most migratory Mid-Atlantic species. The March survey coincides with the spring federal survey, to provide a direct comparison. The November through March sampling programs, when coupled with the winter federal survey that takes place in February, provide near-monthly data on fish distributions in selected areas of the outer continental shelf during the fall-winter-spring transition.

The Supplemental Finfish Survey samples fixed transects oriented parallel to and just north of Baltimore Canyon (38° 20′N) and parallel to and just east of Hudson Canyon (72°W) on all cruises (Figure 1). In January and March, sampling is expanded to include transects west of Alvin Canyon (73° 20′N) and south of Poor Man's Canyon (37°50′N) (Figure 1), weather permitting. Funding permitting, the November and May surveys can also be expanded to four transects. As each mission is constrained by the number of days-at-sea funded, sampling is prioritized: Hudson, Baltimore, Poor Man's, Alvin. As each of the transects is located parallel to and relatively near these canyons, for convenience the transects are given the canyon names as monikers.

Stations are distributed perpendicular to the average trend of the depth contours. A 2:1 ratio of fixed to adaptive stations are occupied on each transect. Fixed stations are located at 40, 50, 60, 80, 100, 125, 150, 200, 225, and 250 fm, unless topography limits sampling. The 250-fm station cannot be sampled on the Baltimore Canyon and Poor Man's Canyon transects, for example. An additional four-to-five adaptive stations, to achieve the 2:1 ratio of fixed to adaptive stations, are distributed along the transects based on the catches of target species recorded at the fixed stations. Target species are summer flounder, scup, black sea bass, monkfish, spiny dogfish, *Loligo* squid, and silver+offshore hake. As of May, 2006, *Illex* squid is added to this set for the May survey only.

To choose adaptive stations, fixed stations providing the highest overall ranking based on the catch of each target species are identified using the following methodology. Let the accent $\rightarrow$ represent the rank of a variable and $\vec{\nu}_{ij}$ represent the rank given to each of the n_f fixed stations, i, for each of the n_t target species, j. As a consequence, each of the fixed stations has a set of n_t rank values, one for each target species, based independently on the catch record for that species among all n_f fixed stations. The adaptive choices are obtained by evaluating the choice variable C_i as the sum of the rank values for each species for that station:

$$C_i = \sum_{j=1}^{n_t} \vec{\nu}_{ij}. \tag{1}$$

The n_f choice variables, C_i, are then ranked and the ranks, $\vec{C}_i$, of each neighboring

Figure 1. Fixed transects are located near major canyons in the Mid-Atlantic. In the original survey design, six fixed transects were to be sampled plus two-to-three adaptive transects chosen two weeks prior to the sampling event. In the 2006 implementation, sampling is limited to the Hudson, Baltimore, Poor Man's, and Alvin Canyon transects. GRA, small-mesh gear-restricted area. Depth in m.

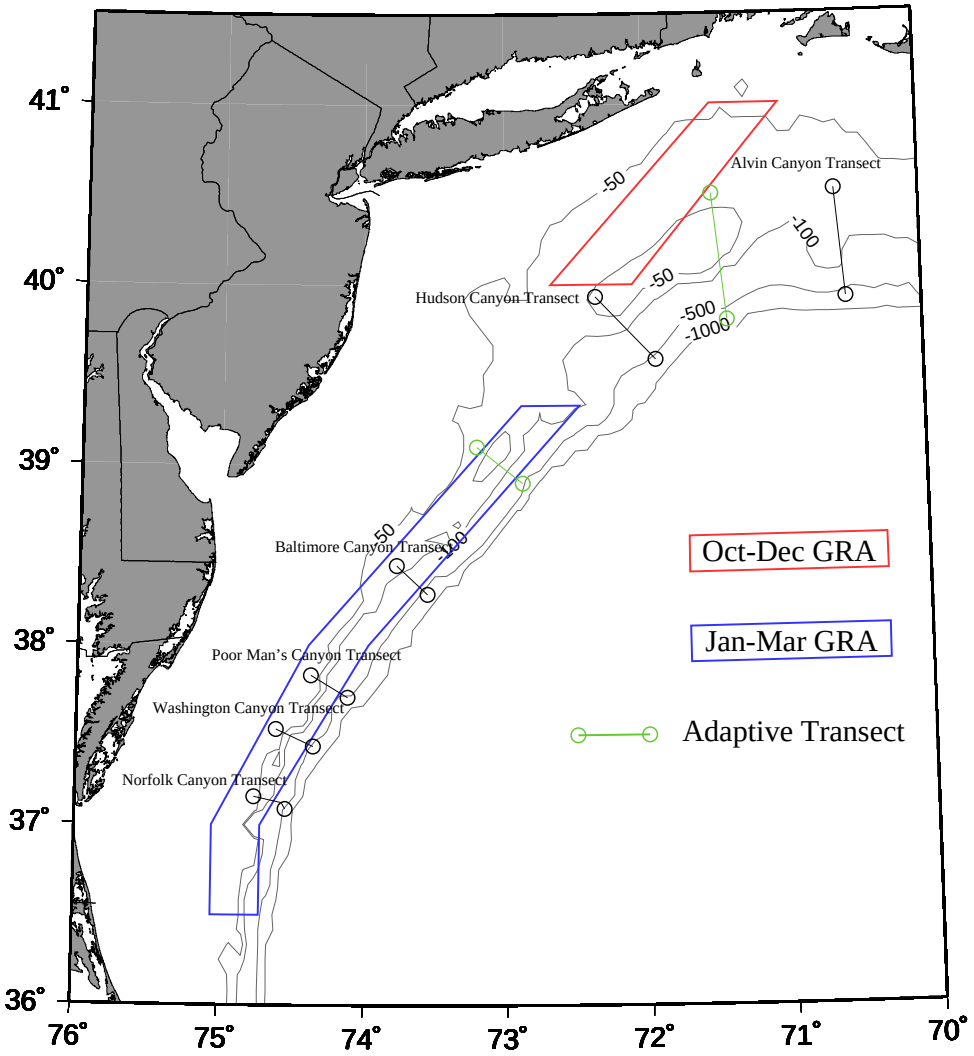

pair averaged:

$$\mathcal{C}_k = \frac{\vec{C}_i + \vec{C}_{i+1}}{2}, \tag{2}$$

where the k are successive averages of fixed station ranks along the transect. There are $n_f - 2$ averaged pairs $\mathcal{C}_k$. Adaptive stations are placed one-half depth increment between fixed station pairs having the highest averaged station ranks, $\vec{\mathcal{C}}_{k=1,4\ or\ 5}$, until all the adaptive stations are allocated for a given transect. The program is

implemented at sea by means of an Excel spreadsheet.

Station Sampling Protocol

Once established, fixed stations are repeatedly occupied at all subsequent time periods (Tables 1 and 2). Site selection for the first occupation of fixed and adaptive stations is made as follows. A specified location is chosen *a priori* based on depth. The vessel steams to that location. The Captain then is permitted to search an area of approximately 1 nautical mile in diameter to identify a satisfactory location for the tow. The tow is oriented alongslope. The direction of the first sampling and the tow locations are retained in all subsequent samplings.

Tow speeds are maintained near 3 knots. Scope is adjusted according to a scope table and varies with depth (Tables 1 and 2), generally falling in the range of 2.5:1 to 3:1. To minimize diel variability, stations in water depths $\leq$150 fm are sampled during daylight hours only. All other stations are sampled at night. Starting and hauling depths, positions, and times and tow warp length are recorded at each station. Depth, door spread, time, and GPS position are logged manually every 5 minutes on the bridge. DGPS position is logged independently electronically to $0.01'$ latitude and longitude every 1 minute during the tow. Depth and bottom water temperature are logged remotely at 1-minute intervals using a *Vemco* sensor attached to the top of the net just behind the headrope.

Some stations may be untowable as originally designed due to lobster pots. A series of modifications are allowed in this circumstance. If a shorter than normal tow can be completed, a shorter tow is taken. If not, an effort is made to relocate the tow within the original 1-nautical-mile radius, first by moving the tow alongslope, then by moving the tow slightly upslope or downslope. If a location is finally judged to be untowable, and the station is a fixed station, that station is dropped from the transect for that survey. If the station is an adaptive station that should be sampled and is untowable, the next ranking adaptive station is used to maintain the desired number of adaptive stations. No stations have been dropped since the survey adopted the present 1-nautical-mile tow length, although occasionally tows have been shortened or moved slightly to avoid fixed gear.

Field Crew

The field crew includes a team of six scientists, plus the Captain and boat crew. The size of the scientific party is limited by berthing space. Science personnel have consistently included four representatives from Rutgers University, including the Chief Scientist, and two from NMFS, normally one from the cooperative research branch and one from the observer program.

Table 1. Start and haul positions and wire out for each target depth on the Alvin and Hudson Canyon transects.

Starting Position		Ending Position		Target	
Latitude	Longitude	Latitude	Longitude	Depth	Wire Out (fm)
Alvin Canyon					
40° 28.946′	70° 34.953′	40° 29.308′	70° 36.276′	40 fm	150
40° 21.615′	70° 36.186′	40° 21.902′	70° 37.620′	50 fm	150
40° 16.805′	70° 35.973′	40° 16.481′	70° 34.585′	60 fm	175
40° 2.720′	70° 36.741′	40° 2.992′	70° 35.333′	80 fm	250
40° 1.824′	70° 35.694′	40° 2.076′	70° 34.275′	100 fm	300
40° 0.745′	70° 34.417′	40° 1.162′	70° 33.077′	125 fm	350
39° 59.693′	70° 34.171′	40° 0.207′	70° 32.894′	150 fm	375
39° 59.169′	70° 30.998′	39° 58.321′	70° 31.825′	250 fm	500
Hudson Canyon					
Fixed Stations					
39° 55.938′	72° 22.183′	39° 54.823′	72° 22.137′	40 fm	150
39° 48.094′	72° 10.494′	39° 48.268′	72° 9.145′	50 fm	150
39° 45.864′	72° 7.321′	39° 45.562′	72° 8.742′	60 fm	175
39° 42.360′	72° 3.280′	39° 41.624′	72° 4.138′	80 fm	250
39° 39.810′	72° 1.050′	39° 40.490′	72° 0.340′	100 fm	300
39° 38.535′	72° 0.075′	39° 39.469′	71° 59.319′	125 fm	350
39° 39.688′	71° 58.077′	39° 40.480′	71° 57.650′	150 fm	375
39° 38.030′	71° 56.980′	39° 37.140′	71° 57.340′	200 fm	450
39° 37.030′	71° 56.540′	39° 37.940′	71° 56.360′	225 fm	475
39° 37.250′	71° 56.070′	39° 36.380′	71° 56.090′	250 fm	500
Adaptive Stations					
39° 53.590′	72° 16.140′	39° 54.630′	72° 16.120′	45 fm	150
39° 45.899′	72° 9.770′	39° 46.284′	72° 8.422′	55 fm	150
39° 41.095′	72° 7.181′	39° 41.970′	72° 6.321′	70 fm	225
39° 39.312′	72° 2.537′	39° 40.160′	72° 2.090′	90 fm	275
39° 40.450′	71° 59.910′	39° 41.060′	71° 59.102′	112 fm	325
39° 37.060′	72° 0.760′	39° 37.900′	71° 59.840′	137 fm	375
39° 37.170′	71° 58.450′	39° 38.090′	71° 57.800′	175 fm	425
39° 38.076′	71° 56.533′	39° 36.892′	71° 56.978′	212 fm	450

Sample Processing Protocol

Sample processing protocol follows standard NMFS survey methods. Each tow is sorted to species and catch weights obtained for each species. Spiny dogfish are separated by sex prior to weighing. For large catches that would take longer than the allotted 3 hours to process, the entire catch is placed in baskets and a subsample of the baskets weighed. If further subsampling is required, subsampling protocols follow NMFS survey methods. Target species for length measurements include: summer flounder, scup, black sea bass, *Loligo* squid, Atlantic mackerel, monkfish, spiny dogfish, skates, *Illex* squid, silver hake, offshore hake, American lobster,

Table 2. Start and haul positions and wire out for each target depth on the Baltimore and Poor Man's Canyon transects.

Starting Position		Ending Position		Target	
Latitude	Longitude	Latitude	Longitude	Depth	Wire Out (fm)
Baltimore Canyon					
Fixed Stations					
38° 22.790′	73° 47.990′	38° 22.090′	73° 48.980′	40 fm	150
38° 22.420′	73° 44.380′	38° 23.050′	73° 43.380′	50 fm	150
38° 22.893′	73° 40.278′	38° 22.076′	73° 41.147′	60 fm	175
38° 17.200′	73° 38.490′	38° 16.350′	73° 39.140′	80 fm	250
38° 16.931′	73° 37.983′	38° 17.853′	73° 37.174′	100 fm	300
38° 16.890′	73° 37.610′	38° 15.763′	73° 37.857′	125 fm	350
38° 16.179′	73° 37.513′	38° 17.167′	73° 36.982′	150 fm	375
38° 15.730′	73° 36.600′	38° 16.690′	73° 36.840′	200 fm	450
38° 17.016′	73° 36.526′	38° 17.126′	73° 35.258′	225 fm	475
Adaptive Stations					
38° 22.270′	73° 46.557′	38° 21.402′	73° 47.534′	45 fm	150
38° 21.969′	73° 43.702′	38° 22.627′	73° 42.653′	55 fm	150
38° 19.438′	73° 39.037′	38° 20.273′	73° 38.191′	70 fm	225
38° 16.470′	73° 38.510′	38° 15.630′	73° 39.100′	90 fm	275
38° 17.740′	73° 36.970′	38° 16.920′	73° 37.730′	112 fm	325
38° 15.820′	73° 38.071′	38° 16.500′	73° 37.520′	137 fm	375
38° 16.368′	73° 37.234′	38° 17.090′	73° 36.660′	175 fm	425
Poor Man's Canyon					
Fixed Stations					
37° 47.474′	74° 19.338′	37° 46.490′	74° 20.124′	40 fm	150
37° 47.351′	74° 17.108′	37° 46.371′	74° 17.785′	50 fm	150
37° 46.630′	74° 14.079′	37° 45.670′	74° 14.769′	60 fm	175
37° 46.948′	74° 10.412′	37° 46.151′	74° 11.367′	80 fm	250
37° 45.238′	74° 11.025′	37° 46.192′	74° 10.291′	100 fm	300
37° 44.650′	74° 10.342′	37° 45.769′	74° 10.255′	125 fm	350
37° 45.343′	74° 10.167′	37° 45.884′	74° 9.185′	150 fm	375
37° 44.991′	74° 9.734′	37° 43.776′	74° 9.177′	200 fm	450
37° 45.354′	74° 9.390′	37° 43.967′	74° 8.863′	225 fm	475
Adaptive Stations					
37° 45.737′	74° 19.012′	37° 46.761′	74° 18.306′	45 fm	150
37° 46.485′	74° 15.904′	37° 45.503′	74° 16.629′	55 fm	150
37° 45.651′	74° 11.126′	37° 46.469′	74° 10.211′	90 fm	275
37° 44.878′	74° 10.697′	37° 45.942′	74° 10.344′	112 fm	325
37° 44.922′	74° 10.234′	37° 45.884′	74° 9.784′	137 fm	375

bluefish, yellowtail flounder, and winter flounder. The goal for each priority species is 100 length measurements for each tow. If fewer than 100 individuals are caught, all of the individuals are measured. Each priority species is divided into size classes and the first three individuals measured in each size class are weighed. Smaller species, such as *Loligo* and *Illex* squid, Atlantic mackerel, silver hake, offshore hake, scup,

and black sea bass, are divided into 5-cm size classes. The larger species, including spiny dogfish, summer flounder, monkfish, bluefish, and large skate species, are divided into 10-cm size classes. If time does not permit sample processing between tows, fish sorted for length measurement are placed in labeled containers and stored in the fish hold until processing can occur. In addition, if time allows, scale and/or otolith samples of large scup, summer flounder, and black sea bass are obtained. A sub-sample of *Illex* squid is frozen at-sea for maturity analysis by NMFS personnel.

Vessel and Gear Information

Surveys are conducted onboard the *F/V Luke & Sarah* (Table 3). The *F/V Luke & Sarah* is 120′ in length with a 1,500 HP engine. To permit efficient capture of groundfish while also maintaining a reasonable degree of catchability for other species such as scup, a 4-seam box net with a standard 6-cm codend (liner) was used. The fishing circle of the net is 506 meshes of 6″ mesh. The extension of the net is 3″ mesh knot to knot, 100 meshes long, and 225 meshes around. The codend is made of 6.5″ mesh knot to knot, 100 meshes long, 70 meshes around, and is lined with a 6-cm mesh liner. The chaffing gear is a mat made of 6″ mesh covering 2/3 of the bottom of the codend. The doors are 104″ Thyboron with a spoiler. Each door weighs 1,640 pounds. The footrope is constructed from 114′ 6.5″ × 1/2″ stainless steel wire wrapped with #12 polyester with two wire extensions of 6′ 5.16″ eye to eye joined with two 3/4″ bow shackles for an overall length of 127′ 11″. The headrope is 117′ 11.52″ overall length, including the extensions. There are 96 8″ hi-impact floats hung in groups of 6 on 5/8″ poly plus, grouped closely together in the center with a set of 6 on each wing. The traveler is made of 1/2″stainless steel wire banded with 1/2″ stainless steel bands to the footrope. The overall length is 119′, with the stainless steel bands spaced at 1′ 11″ intervals. The sweep is made up of 5/8″ stainless steel wire with 84 1.4 pound leads in the center section and 3 link 1/2″ trix drop chains at 1′ 11″ intervals throughout. The sweep is in three sections joined with 1/2″ hanging locks and 2′ 6″ of 1/2″ trix chains on each wing end. Each wing is 46′ 6.84″ eye to eye and the bosom is 29′ 2.28″ eye to eye. The sweep is covered with 3″ rubber cookies.

In November, 2005, the survey ordered a set of survey gear of identical design. Preliminary testing of this new gear in March, 2006, indicated sufficient divergence in catchability to prevent its immediate use. Additional tests will be conducted in November, 2006. Through that time, all surveys will utilize the original survey gear.

Database Content and Configuration

As of April, 2006, all survey data had been provided to NMFS-NEFSC

Table 3. A comparison of vessel characteristics between the *F/V Luke & Sarah* and the *F/V Jason & Danielle*.

	F/V Luke & Sarah	*F/V Jason & Danielle*
Construction Type	Steel	Steel
Length	120′	93′
Engine	1,500 HP @ 1,800 RPM	1,080 HP @ 1,800 RPM
Gross Tonnage	196 tons	176 tons
Hold Capacity	240,000 lbs	150,000 lbs
Winch Wire	7/8"	7/8"
Clutch Ratio	5:1	6:1
Wheel	71" wheel / 72" nozzle	79" open wheel
Net Sensor Package	ITI Simrad	ITI Simrad

(Table 4). A cruise report released to the public has accompained each data transmission*. The methods of calculation for variables listed in the following sections as 'calculated' are given in a section succeeding the sections rendering the file formats. Survey data are provided in the following file formats.

Bridge File Format

The file containing data on tow conditions recorded by hand on the bridge is named: TripID//'captinfo'//month//year.csv, where '//' is the concatenation symbol. For example, the March, 2003, data are found in R01003captinfo0303.csv. The trip identification code is patterned after the codes used by the observer program. Trip identification codes for surveys through May, 2006 are found in Table 4.

The file contains the following fields entered in column format.

1. Trip identification number (scientist identification number//trip number).
2. Tow number (sequential for the entire trip, not by transect).
3. Time (HH:MM, in GMT daylight or GMT standard).
4. Latitude (degrees, decimal minutes).
5. Longitude (degrees, decimal minutes).
6. Depth (m).
7. Bottom temperature (°C – bottom temperature was recorded on the bridge during the March, 2003, survey only).
8. Door spread (m).
9. Surface temperature (°C).

* Cruise reports in pdf format are available from HSRL and NFI-SMC upon request.

Table 4. Summary table of work completed to date on each transect.

Sampling Event	Transect	Number of Stations Sampled	Daytime: Nighttime Adaptive Stations	Cruise Report Released/Data Transmitted to NMFS	Trip ID
March 8-12, 2003	Hudson	13	3:1	October 2003	R01003
	Baltimore	12	4:0		
May 25-29, 2003	Hudson	15	4:1	November 2003	R01005
	Baltimore	13	4:0		
Jan. 24-Feb. 2, 2004	Hudson	15	4:1	July 2004	R05001
	Baltimore	9	0:0		
March 4-17, 2004	Hudson	14	4:0	October 2004	R05003
	Baltimore	13	3:1		
	Poor Man's	10	2:0		
May 19-23, 2004	Hudson	13	3:0	December 2004	R05005
	Baltimore	9	0:0		
November 15-21, 2004	Hudson	15	5:0	March 2005	R05007
	Baltimore	13	3:1		
January 10-22, 2005	Hudson	15	4:1	June 2005	R05001
	Baltimore	13	3:1		
March 13-23, 2005	Alvin	8	0:0	September 2005	R05003
	Hudson	15	4:1		
	Baltimore	13	3:1		
	Poor Man's	13	4:0		
May 4-10, 2005	Hudson	15	4:1	November 2005	R05005
	Baltimore	13	4:0		
November 10-16, 2005	Hudson	15	3:2	April 2006	R05006
	Baltimore	13	4:0		
January 19-31, 2006	Hudson	15	3:2	In Progress	R08001
	Baltimore	13	3:1		
	Poor Man's	13	4:0		
March 1-14, 2006	Hudson	15	4:1	In Progress	R08002
	Baltimore	13	3:1		
	Poor Man's	13	3:1		
May 3-9, 2006	Hudson	15	5:0	In Progress	R08003
	Baltimore	13	3:1		

Vemco Temperature/Depth File

The *Vemco* minilogger records temperature and depth information logged at 1-min intervals and is named: TripID//'minilog'//month//year.csv. For example, R05003minilog0304.csv contains the *Vemco* data from the March, 2004, survey. This is a raw minilogger file and, consequently, has a series of header lines that are output directly from the *Vemco* minilogger, the last of which contains the column fields.

The file contains the following fields entered in column format.

1. Trip identification number (scientist identification number//trip number).
2. Date (MM/DD/YY based on EST daylight or EST standard – the November, 2004, survey was recorded in GMT standard).
3. Time (HH:MM:SS, EST daylight or EST standard – the November, 2004, survey was recorded in GMT standard).
4. Temperature (March 2003-November 2004 surveys, °F; January 2005-November 2005 surveys, °C).
5. Depth (m), annotated to identify the starting and ending position of each tow.

Position File

DGPS position is recorded at 1-min intervals using *P-Sea Windplot* software and given the following name: TripID//'track'//month//year.csv. For example, March, 2003, position data can be found in R01003track0303.csv. This file is a raw datalogger file.

The file contains the following fields entered in column format.

1. Trip identification number (scientist identification number//trip number).
2. Tow number (sequential for the entire trip).
3. Latitude (degrees, decimal minutes).
4. Longitude (degrees, decimal minutes).
5. Time (HH:MM:SS, EST daylight or EST standard).

Station File

Information about the vessel, gear, and some data describing each tow can be found in the station file named: TripID//'station'//month//year.csv. The file, R05003station0305.csv, for example, contains trip information from the March, 2005, survey.

The file contains the following fields entered in column format.

1. Tow number (sequential for the entire trip).
2. Trip identification number (scientist identification number//trip number).
3. Vessel name (8 character maximum).
4. Vessel hull number.
5. Date landed (MM/DD/YY, based on EST daylight or EST standard).
6. Codend mesh size (mm).
7. Target species. (SummerFlou is entered in this field as an example target species, although this is a multispecies survey, and seven other target species, for the adaptive station algorithm, are included.)
8. Tow date (MM/DD/YY, based on EST daylight or EST standard).

9. Set latitude (degrees and decimal minutes, as recorded on the bridge).
10. Set longitude (degrees and decimal minutes, as recorded on the bridge).
11. Haul latitude (degrees and decimal minutes, as recorded on the bridge).
12. Haul longitude (degrees and decimal minutes, as recorded on the bridge).
13. Set depth (m, as recorded on the bridge).
14. Haul depth (m, as recorded on the bridge).
15. Number of data lines for that tow in the catch file (equivalent to the number of species caught during the tow)
16. Set time (HH:MM, as recorded on the bridge, EST daylight or EST standard).
17. Haul time (HH:MM, as recorded on the bridge, EST daylight or EST standard).
18. Headrope length (m).
19. Footrope length (m).
20. Ground cable length (m).
21. Tow wire out (m).
22. Tow speed (km h^{-1}, as estimated on the bridge).
23. Station type (f=fixed, a=adaptive).
24. Transect (h=Hudson Canyon, b=Baltimore Canyon, p=Poor Man's Canyon, a=Alvin Canyon).
25. Total number of stations sampled during the trip.
26. Target depth (m, determined pre-cruise, standardized across all surveys).
27. Surface temperature (°C, calculated as the average temperature recorded by the *Vemco* minilogger immediately after the net enters the water and immediately before the net leaves the water).

Tow File

A summary of the remaining tow information is recorded in the file named: TripID//'towdata'//month//year.csv. For example, R05001towdata0105.csv contains data from the January, 2005, survey. *Note that target depth, not tow number, identifies the sequence of stations along the transect. Tow number identifies the sequence of stations during the survey.*

The file contains the following fields entered in column format.

1. Trip identification number (scientist identification number//trip number).
2. Transect (h=Hudson Canyon, b=Baltimore Canyon, p=Poor Man's Canyon, a=Alvin Canyon).
3. Tow number (sequential for the entire trip).
4. Tow date (MM/DD/YY, based on EST daylight or EST standard).
5. Target depth (m, determined pre-cruise – tows are aligned along the transect by ranking them by target depth, not by tow number)
6. Average depth (m, calculated from *Vemco* minilogger data).

7. Depth range (m, calculated from *Vemco* minilogger data).
8. Scope (unitless, calculated).
9. Swept area (km^2, calculated).
10. Swath area (km^2, calculated).
11. Bottom temperature (°C, calculated from *Vemco* minilogger data).
12. Tow time (h, calculated).
13. Average tow speed (km h^{-1}, calculated).
14. Tow distance (km, calculated).

Species Catch File

The file containing the species code, name, and catch data for each species is named: TripID//'catch'//month//year.csv. An example file from the May, 2005, survey is R05005catch0505.csv.

The file contains the following fields entered in column format.

1. Trip identification number (scientist identification number//trip number).
2. Tow number (sequential for the entire trip).
3. Survey code (the NMFS survey species code – if a species was caught that does not have a survey code, then the observer code was assigned; species with neither a survey nor an observer code were assigned a code of 978-994).
4. Sex code (0=not sexed, 1=male, 2=female).
5. Species name (common name associated with the survey code – if a species was subsampled by size, then the size category is identified in the name).
6. Total catch (kg).
7. Sample weight (kg, weight of measured individuals – a sample weight of zero means that lengths were not measured for the species in that tow).

Length File

The length data are in a file named: TripID//'length'//month//year.csv. For example, R05006length1105.csv contains the length data from the November, 2005, survey.

The file contains the following fields entered in column format.

1. Trip identification number (scientist identification number//trip number).
2. Tow number (sequential for the entire trip).
3. Survey code (the NMFS survey species code – if a species was caught that does not have a survey code, then the observer code was assigned; species with neither a survey nor an observer code were assigned a code of 978-994).
4. Sex code (0=not sexed, 1=male, 2=female).

5. Fork length (cm, with two exceptions – for American lobster, the carapace is measured in mm; for skates, the total length [tip of upper snout to end of tail] is measured).
6. Number of individuals at that length for the tow.
7. Size category name (blank except in instances where a single species was subsampled by size group).

Weight File

The individual lengths and weights of weighed fish are recorded in a data file named: TripID//'indfish'//month//year.csv. For example, R05005indfish0504.csv contains the data from the May, 2004, survey.

The file contains the following fields entered in column format.

1. Trip identification number (scientist identification number//trip number).
2. Tow number (sequential for the entire trip).
3. Survey code (the NMFS survey species code – if a species was caught that does not have a survey code, then the observer code was assigned; species with neither a survey nor an observer code were assigned a code of 978-994).
4. Individual identification number unique to each weighed fish, assigned consecutively in the file.
5. Fork length (cm, with two exceptions – for American lobster, the carapace is measured in mm; for skates, the total length [tip of snout to end of tail] is measured).
6. Individual weight (kg).

Method of Calculation of 'Calculated' Variables

In the following, the tilde accent is used to refer to the mean of all values of a variable obtained during a given tow. Thus, the average depth, $\tilde{z}$ (in m) for the tow is calculated as:

$$\tilde{z} = \frac{\sum_{i=1}^{n_z} z_i}{n_z} \tag{3}$$

where n_z is the total number of depth recordings taken at 1-min intervals by the *Vemco* minilogger during the tow.

Average bottom temperature, $\widetilde{T}_B$, is the average of the temperature recordings taken at 1-min intervals by the *Vemco* minilogger during the tow.

Tow distance, D in km, is determined from the GPS positions between the positions assigned for net-on-bottom and net-off-bottom, by summing the n_δ 1-min

distance segments, δ, between these two events.

$$D = \sum_{i=1}^{n_\delta} \delta_i. \tag{4}$$

Tow time, $\mathcal{T}$ in hr, is determined from the *Vemco* depth recorder as the difference between the time of bottom contact (net-on-bottom) and haul back (net-off-bottom). These events are determined by changes in *Vemco* sensor depth recorded at 1-min intervals. As a consequence, the uncertainty in tow time $\mathcal{T}$ and tow distance D is approximately $\left(\frac{\leq 2 min}{T} \leq 10\%\right)$.

Depth range, DR in m, is calculated for each tow as:

$$DR = max(z_i) - min(z_i), \ for\, i = 1, n_z. \tag{5}$$

Scope (unitless) is calculated as the ratio of wire out (W in m) to average depth (m):

$$Sc = \frac{W}{\tilde{z}}. \tag{6}$$

Average tow speed, Sp in km hr^{-1}, is calculated from tow distance and time:

$$Sp = \frac{D}{\mathcal{T}}. \tag{7}$$

Average door spread, $\widetilde{Ds}$ in m, is calculated from the 5-min notations taken on the bridge during the tow.

Swept area, SWP in km^2, is calculated from distance traveled and door spread and, thus, represents a maximum value for swept area:

$$SWP = D\,\widetilde{Ds}. \tag{8}$$

Swept area biomass, B_{SWP} in kg km^{-2}, is then:

$$B_{SWP} = \frac{C}{SWP} \tag{9}$$

where C is species catch weight (in kg).

The Supplemental Finfish Survey is transect based, with one tow taken per target depth on each transect. As such, the transect can be modeled as a series of conterminous strata with a sampling density of one sample per stratum. These strata are the width of the sampling gear, $\widetilde{Ds}$. The length of each stratum varies according to the slope of the shelf and can be evaluated based on information depicted in Figure 2.

Referring to Figure 2, let $\dot{E}$ represent the dropped-perpendicular position of the

Figure 2. Cartoon showing the mapping of tows onto the backbone transect line and the calculation of swath distance, the linear distance allotted to each tow had it actually been taken along the transect line. Assignment of linear distance is based on the geometry of two right triangles whose common side is defined by the midpoint of the tow and the intersection of a perpendicular dropped from the midpoint to the backbone transect line.

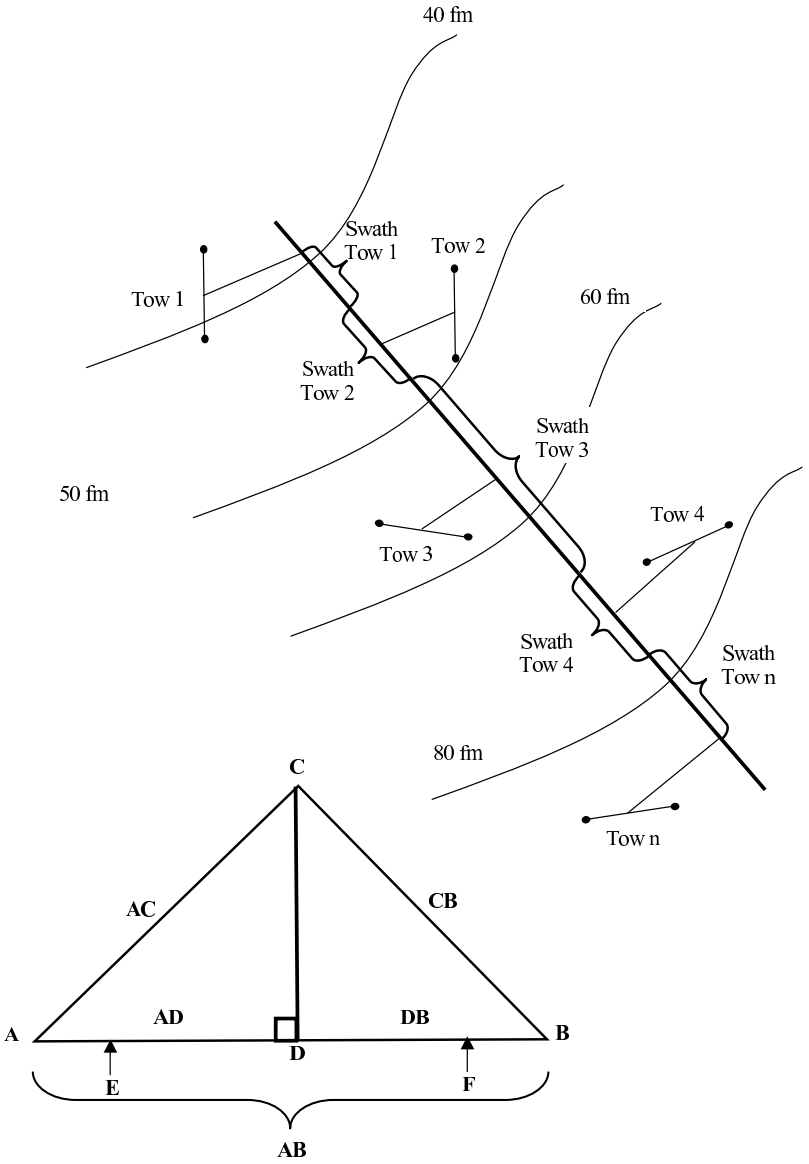

preceding tow on the backbone transect line; $\dot{F}$, the dropped-perpendicular position of the succeeding tow on that line, and $\dot{D}$, the dropped-perpendicular position of the tow in question, obtained by dropping a perpendicular from the mid-point of a tow, located at $\dot{C}$, to the backbone transect line. Let $\overline{AB}$ define the backbone transect

line perpendicular to the depth contours of the sampled region[‡]. This geometry is necessitated by the fact that tows, due to local topographic constraints, cannot be sited so that their midpoints fall precisely on the backbone transect line.

Accordingly, the desired linear distance, $\mathcal{L}$, along the transect backbone, equivalent to the stratum length, apportioned to the tow with midpoint $\dot{C}$ is:

$$\mathcal{L}_{\dot{C}} = \frac{\overline{ED}}{2} + \frac{\overline{DF}}{2}. \tag{10}$$

Any given distance segment along the backbone $\overline{AB}$, such as $\overline{ED}$, is obtained by calculating and summing line segments sequentially from a point upslope of the shallowest sampled station (40 fm), $\dot{A}$ in Figure 2, such that

$$\overline{ED} = \overline{AD} - \overline{AE} \tag{11}$$

where $\overline{AE}$ is a previously calculated distance. $\overline{AD}$ is obtained by recognizing that:

$$\overline{AC}^2 = \overline{AD}^2 + \overline{CD}^2 \tag{12}$$

$$\overline{BC}^2 = \overline{BD}^2 + \overline{CD}^2 \tag{13}$$

and

$$\overline{AB} - \overline{AD} = \overline{BD}. \tag{14}$$

Solving equations (13), (14), and (15) for $\overline{AD}$ yields:

$$\overline{AD} = \frac{\frac{\overline{AC}^2 - \overline{BC}^2}{\overline{AB}} + \overline{AB}}{2} \tag{15}$$

Swath area, SWT in km^2, or the area of any stratum i associated with a given tow, is then the linear distance times the average door spread:

$$SWT_i = \mathcal{L}_i \widetilde{Ds}_i. \tag{16}$$

Swath area biomass, B_{SWT_i} in kg, or the biomass estimated for a given depth stratum i along the transect line, is the multiple of the swept-area biomass and the swath area:

$$B_{SWT_i} = B_{SWP_i} SWT_i. \tag{17}$$

In effect, swath area biomass, B_{SWT}, measures the relative importance of each sampled depth according to its contribution to total linear distance along the transect set perpendicular to the average depth contour. The biomass per swept area can then be expanded to estimate the domain biomass, B_T, defined by the

[‡] Note that the two positions defining the backbone transect, $\dot{A}$ and $\dot{B}$, are unimportant as long as $\dot{A}$ is upslope of the first (40 fm) station and $\dot{B}$ is downslope of the last (250 fm) station and $\overline{AB}$ is perpendicular to the depth contours with a peregrination through the region from which the tows were taken.

sum of the swath areas of the n_s conterminous strata defining the transect:

$$B_T = \sum_{i=1}^{n_s} B_{SWT_i}. \tag{18}$$

Historical Review of Survey Protocol Changes

Original Survey Design

The survey began with a planning workshop in Woods Hole at NMFS-NEFSC on January 16, 2003, attended by representatives from Academia, the NMFS, the MAFMC, and the fishing industry. Out of this workshop came the design for a full-scale supplemental survey and a plan for a pilot program for 2003 to test and improve survey protocols. Field efforts occurred in March and May of that year and have occurred four times per year thereafter. Retrospective and planning meetings bounded each cruise for the first two years, usually in association with the MAFMC/NEFSC Trawl Survey Advisory Committee, and have occurred at least twice yearly thereafter. The retrospective and planning meetings have been carried out by an *ad hoc* working group[†] established initially to develop the basic survey design and to introduce improvements during the 2003 pilot year. This *ad hoc* working group has continued to meet to evaluate survey performance and adopt modifications to survey protocols. A summary of these modifications is provided by Figure 3 and Table 5. Field protocols have been refined by this process and are now stabilized.

The original survey design envisioned an 8- or 9-transect survey four times yearly. In this full-scale survey, an adaptive design would be used such that six of the transects would be fixed and two to three would be redistributed for each survey according to (1) information obtained from the fishing industry concerning observed concentrations of target species about two weeks prior to the survey and (2) near-term information on temperature gradients. Fixed transects were to be sited parallel to major canyons: Norfolk, Washington, Baltimore, Poor Man's, Hudson, and Alvin (Figure 1). Locations for an additional, minimally two, transects were to be chosen at a pre-cruise meeting prior to each field program. Funding has limited the scale of the transect sampling to maximally four transects, with a minimum of two sampled four times yearly.

Besides the limitation on the number of transects sampled, all other aspects of the original survey design were implemented. Modifications thereafter occurred to improve upon the original design. These are summarized in Figure 3 and Table 5 and detailed in a subsequent section.

[†] Core members of the *ad hoc* working group include the authors, Russell Brown (NEFSC), Jim Ruhle (MAFMC), Phil Ruhle (Industry), Hank Lackner (Industry), and Paul Perra (NERO).

Figure 3. The number of changes made to sampling protocols over the course of the survey, as summarized in Table 5.

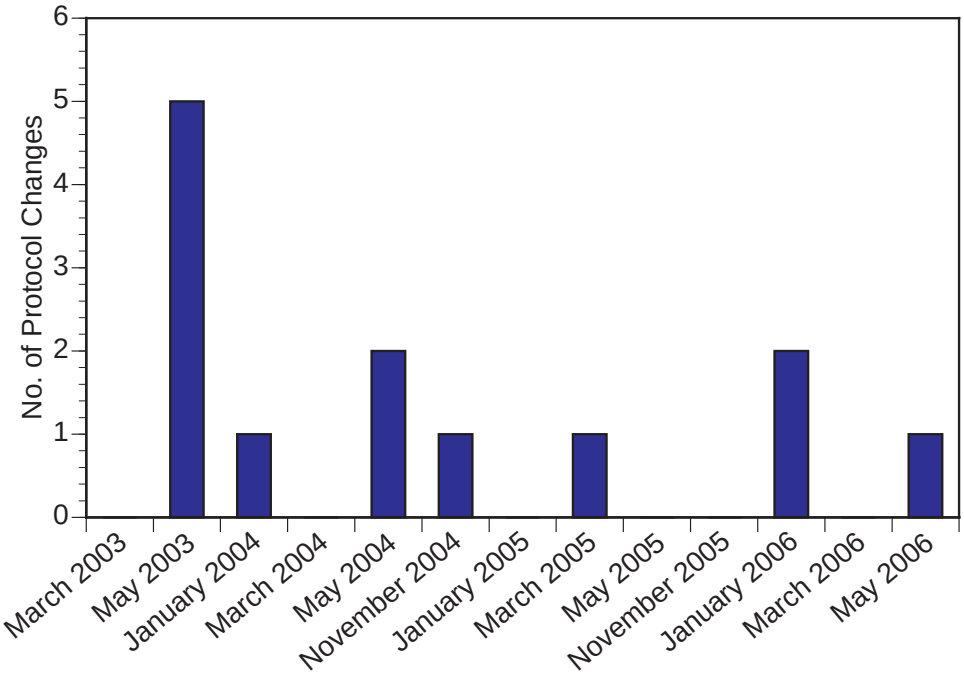

The survey is now in its fourth year. To date, thirteen field programs have been completed (Table 4). The first survey took place on the *F/V Jason* & *Danielle* from March 8-12, 2003. A total of 25 tows were made along the Hudson and Baltimore Canyon transects during the March survey and 28 tows during the week of May 25-29, 2003, thereby establishing the first May survey (Table 4). In 2004, the survey was expanded with field programs in January and November, as well as March and May. Sampling occurred on the Baltimore and Hudson Canyon transects during the weeks of January 24-February 2, March 4-17, May 19-23, and November 15-21 (Table 4). In addition, a transect near Poor Man's Canyon was sampled during the March, 2004, survey. A new transect sited near Alvin Canyon was established during the March, 2005, survey. Thus far in 2006, three surveys have been completed on the Hudson, Baltimore, and Poor Man's Canyon transects during the weeks of January 19-31 and March 1-14 and on the Hudson and Baltimore Canyon transects during May 3-9.

Survey Protocol Modifications

Overall, the majority of changes in survey design and sampling protocols occurred during the first two years of the program (Figure 3), with the largest number made after the first field program in March, 2003. No changes that have gone into effect since the beginning of the 2005 field season can have any impact on

Table 5. A summary of the changes in survey protocol tabulated in Figure 3.

Date	Protocol Change
May, 2003	1. 40-fm station added to the fixed station list; by definition, a 45-fm adaptive station also added. 2. *Loligo* squid and silver+offshore hake included in the adaptive station selection algorithm. 3. 60-fm tow repositioned on Baltimore Canyon transect. 4. Silver hake and offshore hake distinguished and sorted separately. 5. Diel-sampling protocol instituted; depths >150 fm sampled at night; depths ≤150 fm sampled during the day.
January, 2004	1. Spiny dogfish sorted by sex.
May, 2004	1. Tow distance reduced to 1 nautical mile. 2. Scope table formulated to maintain constant scope at a given depth.
November, 2004	1. *F/V Luke & Sarah* becomes survey vessel.
March, 2005	1. Poor Man's Canyon transect repositioned.
January, 2006	1. *Illex* squid samples for maturity analysis added to biological sampling protocol. 2. Atlantic mackerel added to the priority species list for length measurement.
May, 2006	1. *Illex* squid added to adaptive station algorithm for May surveys only.

catchability.

Numerically, the largest number of changes in survey protocol occurred after the first field program in March, 2003 (Table 5). A fixed station was added at 40 fm on all transects to increase sampling intensity. As a consequence, a 45-fm adaptive station was also added. The 60-fm station on the Baltimore Canyon transect was repositioned because the March location was more than 1 nautical mile from the main transect line. Since *Loligo* squid and silver+offshore hake are commercially important species, they were included with summer flounder, scup, black sea bass, monkfish, and spiny dogfish as target species used to determine the location of adaptive stations. Silver hake and offshore hake, being very similar species, were not separated to species adequately in March, 2003. Subsequent training of survey crew corrected this inadequacy beginning in May, 2003. Catches for the two species are combined in the March, 2003, dataset.

The most important change in protocol after the March, 2003, field program was the decision to sample stations in water depths ≤150 fm during daylight hours

and to sample deeper stations at night. This change originated in the recognition that a number of important species, such as *Illex* and *Loligo* squid (NEFSC, 2002) and silver hake (NEFSC, 2006) undergo diel migrations and that sample number on any given transect was not sufficient to treat diel variability as a random variable. As a consequence, beginning in May, 2003, day-night sampling was rigorously fixed according to depth. This modification to sampling routine has several implications. First, the 175-fm adaptive station is unique in that this is the only station with a fixed station upslope sampled during the day and a fixed station downslope sampled at night. The 175-fm adaptive station itself is sampled at night. All other adaptive stations are bounded by fixed stations sampled in the equivalent diel period. Second, the implementation of the diel-sampling rule adds a complication to at-sea logistics in that adaptive stations may require additional time on each transect because only a subset of them can be sampled in the same diel time period. The value of adaptive stations, accordingly, for increased accuracy of biomass estimates, cross-shelf distributional patterns, and improved size-frequency estimates must outweigh the decrease in total sample number per day-at-sea necessitated by this approach. The degree of catch bias incurred in underestimating diel migratory species at night at the deeper stations has not been evaluated.

Beginning in January 2004, spiny dogfish were separated by sex prior to analysis. The spiny dogfish assessment focuses on females, so that this modification was designed to increase the usefulness of survey data in the assessment process.

In May, 2004, tow distances were reduced from a fixed distance of two nautical miles to a fixed distance of one nautical mile, in order to minimize sub-sampling, reduce on-deck processing time and thus, increase the number of stations that can be sampled during the survey. This later was the principal consideration, as large catches, particularly in January and March, reduced significantly the total number of stations and transects that could be occupied. Previous studies indicate that towing for longer than 15 minutes at a station generally does not gain much in precision and is often not practical due to the high cost of at-sea operations (e.g., Pennington and Vølstad, 1991; Folmer and Pennington, 2000). Along with a change in vessel, the change in tow time is one of two modifications in sampling protocol subsequent to May, 2003, capable of significantly impacting biomass estimates. A detailed evaluation follows in a subsequent section.

Scope was set in March 2003 by the captain of the *F/V Jason & Danielle* to obtain best fishing performance for the survey gear, based on the Captain's intimate knowledge of the gear's performance over a range of depths. The Captain was allowed to repeat this choice for each of the subsequent four surveys (May, 2003, November, 2003, January, 2004, and March, 2004). In May 2004, in order to maintain a consistent towing strategy and minimize variability in net geometry, a scope table (Tables 2 and 3) was established using the average scope values for

each depth from the four field programs following March 2003. March, 2003 was excluded due to the unrepresentativeness of this first field program, as detailed subsequently. This table has been used in all surveys since March, 2004, to specify a fixed amount of wire to be paid out at each target depth.

In the summer of 2004, the *F/V Jason & Danielle* was sold and converted to a scallop dredge vessel before a new survey vessel could be calibrated. Beginning with the November 2004 survey, all sampling efforts have been conducted on the *F/V Luke & Sarah* using exactly the same net, doors and sampling protocols. The Captain of the *F/V Jason & Danielle*, Hank Lackner, served as Captain of the *F/V Luke & Sarah* for the first two subsequent surveys to provide on-vessel training for the Captain and crew of the *F/V Luke & Sarah*. The *F/V Luke & Sarah* is of the same design as the *F/V Jason & Danielle*, originally being of the same size and tonnage. The vessel was 'stretched' some years after original construction and is now somewhat larger than the *F/V Jason & Danielle* (Table 3).

In March, 2005, due to a steep depth gradient at deepwater stations, the large boulders present at the original survey locations, and a vessel foundering that occurred a few months prior that prevented resampling the shallow end of the original transect, the Poor Man's Canyon transect was repositioned approximately 15 km south of its original location.

In January, 2006, *Illex* was added to the biological sampling protocol. A subsample of *Illex* squid was frozen at-sea to be processed by NMFS-NEFSC personnel for maturity analysis. To expand the use of the survey as a possible pre-season survey for *Illex* squid, *Illex* squid was added to the species list for the adaptive station algorithm for May only. this modification was first implemented in May, 2006. Also, Atlantic mackerel was added to the list of priority species for length measurements, beginning in January, 2006.

Gear Purchases

Two new codends were built solely for the Supplemental Finfish Survey and were first used in November, 2004. These codends have been used for all subsequent field efforts. These codends were built by *Gearwork & Marine Supply, Inc.*, to the same specification as those used during previous surveys. In winter, 2005, orders were placed for a second set of survey gear, including net and doors. This gear was built by *Trawlworks, Inc.* and arrived for testing in March, 2006. As of this writing, the new gear awaits further testing in November, 2006, before being used for survey sampling.

Reproducibility of Survey Sampling Protocols

Perspective and Methods

In the following discussion, emphasis is placed on identifying survey transect datasets that differ significantly from the majority of survey transect datasets. We treat each transect from each survey as an independent dataset in the following analyses, hereafter referred to as survey-transects. From the summary of survey changes provided in Figure 3, one can expect at least four sources of variation. Since the inception of the survey, three significant modifications in survey sampling protocol have occurred which may impact the representativeness of the data obtained. The first major change occurred when tow distance was reduced from 2 nautical miles to 1 nautical mile. The second was the change in survey vessel. The third was the improvement in a number of survey protocols subsequent to the first field program in March, 2003, including the introduction of the diel-sampling rule, that should imbue the March, 2003, survey with some unique characteristics. Finally, some variations may occur for reasons not anticipated from these major changes in the sampling program. The majority of this latter group will be shown to originate in electronic sensor malfunctions. Statistical analysis will emphasize sampling metrics: tow distance, tow time, average tow depth, depth range, scope, swept area, tow speed, and average door spread. The analysis is impeded by the confounding of time with these changes in protocol, simultaneous comparisons are not available, and because the number of replicate surveys per season is small. Thus seasonal variations cannot normally be distinguished from other sources of variation with statistical robustness and changes due to variations in sampling protocol can never be distinguished from temporal changes in fish availability with surety.

Depth, depth range, and scope depend upon the target depth and therefore, to evaluate differences among surveys for these variables, we first standardize them by calculating the residuals, computed as the difference between the observed value and the mean at each depth, and standardize the residual by depth. The mean used to calculate the residual is derived from all tows at that target depth across all survey-transects. For example, for a given depth j and tow i

$$Standardized\,Residual_{ij} = \frac{\frac{\sum_{i=1}^{n} observed_{ij}}{n} - observed_{ij}}{Target\,Depth_j}. \tag{19}$$

The set of sampling metrics includes a number that can be expected to be correlated to some, often to a large, degree. Consequently, Principal Components Analysis (PCA) is employed to organize the metrics into meaningful groups and to limit the number of statistical comparisons. PCA was conducted on variables first standardized to a mean of zero and a standard deviation of one. As the purpose of the analysis is to include all tow metrics, Factors 1-6, that describe 99% of the variability, are included in the analysis. Factor loads are rendered in Table 6.

Statistical analysis of factor scores was carried out by ANOVA with survey-transect as the independent variable. *A posteriori* Tukey's Studentized Range Tests were used to identify sources of variation within significant ANOVAs.

Table 6. Eigenvalues and factor loads obtained from PCA using the tow metrics: tow distance, tow time, average tow depth, depth range, scope, swept area, tow speed, and average door spread. For depth, depth range, and scope, the depth-standardized residual for each observation was calculated as the difference in a given station value and the overall mean for that station across all surveys standardized to target depth.

Variable	Factor 1	Factor 2	Factor 3	Factor 4	Factor 5	Factor 6
Eigenvalue	3.49	1.49	1.09	1.00	0.49	0.43
.....						
Door spread	0.04	0.99	0.02	0.02	-0.06	-0.08
Residual of Depth	-0.16	-0.07	0.29	-0.04	0.94	-0.01
Residual of Depth Range	-0.03	0.02	-0.01	1.00	-0.03	0.01
Residual of Scope	-0.04	0.02	0.96	-0.01	0.27	0.01
Swept Area	0.94	0.18	-0.02	-0.00	-0.09	0.25
Tow Time	0.99	-0.03	-0.03	-0.03	-0.09	0.07
Tow Speed	0.45	-0.11	0.01	0.02	-0.01	0.88
Tow Distance	0.96	-0.05	-0.03	-0.02	-0.08	0.27

The factor loads show that swept area, tow time, and tow distance are highly correlated as expected and fall on Factor 1. Factor 2 carries the variable door spread; Factor 3, the depth-standardized residual of scope; Factor 4, the depth-standardized residual of depth range; Factor 5, the depth-standardized residual of depth; and Factor 6, tow speed. Tow speed is unique in loading relatively strongly on two factors, Factor 6 and Factor 1.

Tow Distance, Tow Time, and Swept Area

Because all of these variables are related to distance, significant differences can be expected between the survey-transect datasets produced by the 1-nm and 2-nm tows (1.852 km and 3.704 km). Not surprisingly, the average factor scores for each of the survey-transect datasets fall into two distinct groups (Figure 4). As anticipated, the survey-transects characterized by 1-nm tows differ significantly in tow distance, tow time, and swept area from the 2-nm tows (ANOVA, $P<0.0001$).

For target tows of 1-nm and 2-nm, mean tow distances ranged from 3.72 to 4.22 km and 1.78 to 2.21 km, respectively. The Tukey's groupings confirm significant differences among surveys and transects. Tows on the Baltimore Canyon transect tended to be slightly longer then tows on the Hudson Canyon transect (Figure 5). Limited data suggest no difference between the two boats. The Tukey's groupings

show minor differences within the two major groups of survey-transects. These minor differences, though significant statistically, represent small differences on a practical basis. Some portion of these differences are due to the occasional shorter tows generated by large catches, more common in the 2-nm datasets, and the distribution of fixed gear. Figure 6 shows the range of tow distances at each target depth sampled. Only a few outlier tows exist. Overall, the survey has been more effective at achieving the target tow distance since the target distance was reduced to 1 nm.

Figure 4. PCA factor plot of of the average factor scores for Factor 1, describing tow distance, tow time, and swept area, versus Factor 3, describing the depth-standardized residual of scope.

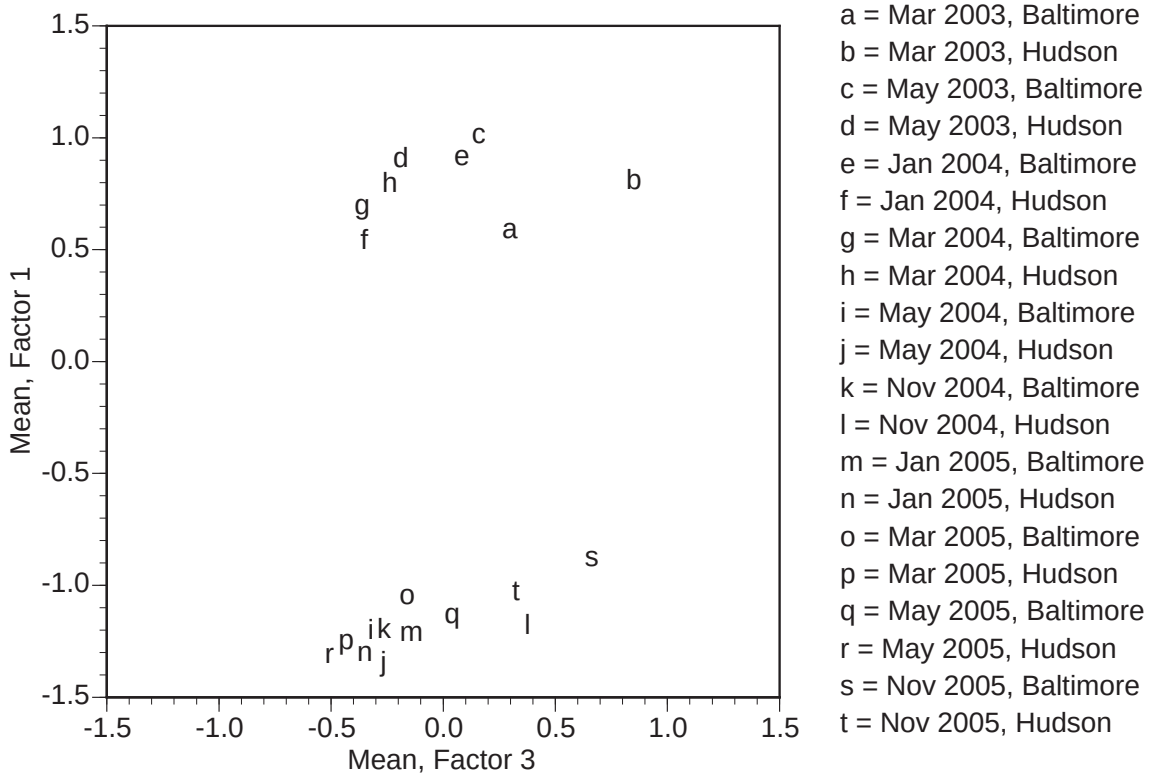

Average tow times ranged from 0.71-0.80 h for 2-nm tows and 0.38-0.43 h for 1-nm tows (Figures 7 and 8). Tow times were more variable when the target distance was 2 nautical miles, because events leading to shorter tows had a higher probability of occurring. Transect differences were not apparent. Based on limited data, a change in vessels did not affect tow time. Time-on-bottom was consistently longer then the target tow time and tows made at deeper stations had a wider range of values (Figure 8). Target tow time is based on target distance and a constant target speed of 3 knots. The observed tow times were, on average, greater then

Figure 5. Mean tow distance (km) and Tukey's grouping for each survey and transect. Blue bars represent trips made on the *F/V Jason & Danielle* and black bars represent trips made on the *F/V Luke & Sarah*. Solid bars represent the Hudson Canyon transect and checkered bars represent the Baltimore Canyon transect. The red line indicates the target value and the horizontal black lines indicate Tukey's grouping where surveys that fall within the same Tukey's grouping are not significantly different at $\alpha = 0.05$.

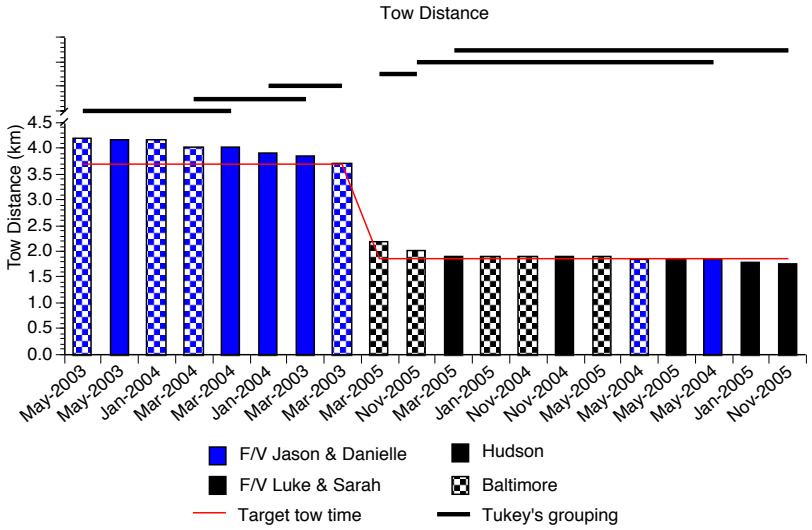

Figure 6. Mean tow distance (km) at each target depth (m) sampled during all surveys. Solid lines represent the target tow distance, that currently is 1 nm but was 2 nm prior to May, 2004.

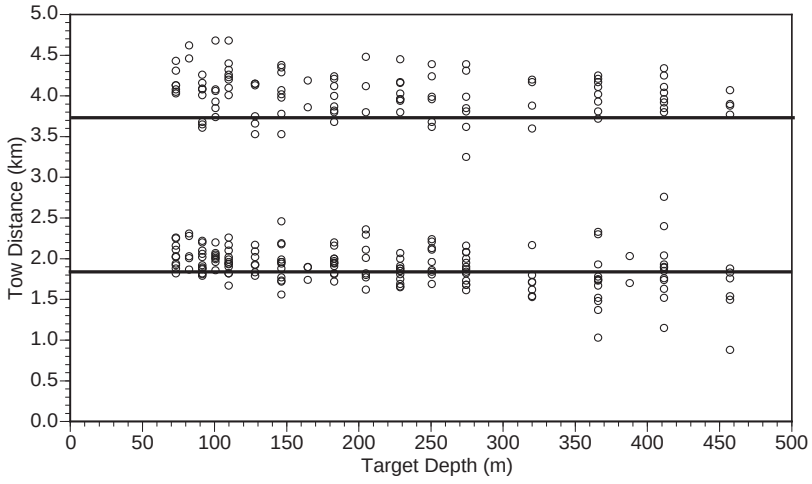

the target because the net remains on the bottom for a few minutes (depending on

depth and the amount of wire paid out) after haulback begins (see also Wallace and West, 2006). The vessel slows down during haulback, thus, lowering average tow speed and extending the time required to achieve the target distance.

Figure 7. Mean tow time (h) for each survey and transect. Blue bars represent trips made on the *F/V Jason & Danielle* and black bars represent trips made on the *F/V Luke & Sarah*. Solid bars represent the Hudson Canyon transect and checkered bars represent the Baltimore Canyon transect. The red line indicates the target value and the horizontal black lines indicate Tukey's grouping where surveys that fall within the same Tukey's grouping are not significantly different at $\alpha = 0.05$.

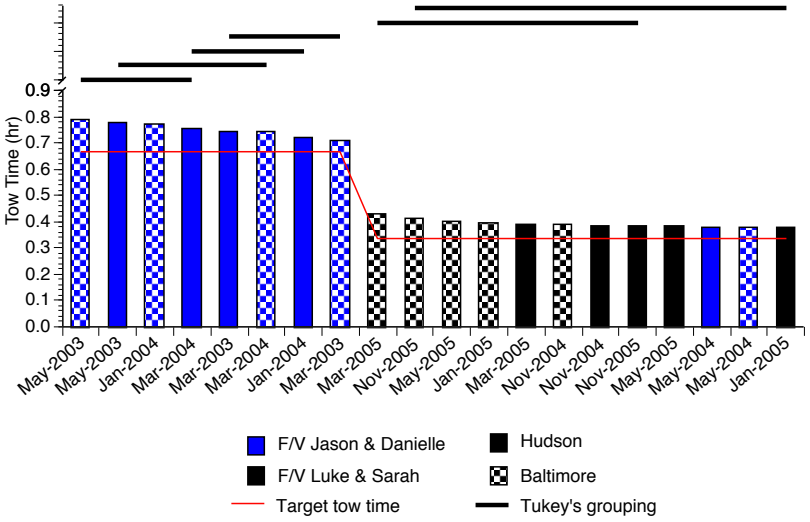

For 2-nm and 1-nm tows, mean swept areas ranged from 0.25-0.29 km^2 and 0.12-0.15 km^2, respectively, and tended to be more variable at deepwater stations (Figures 9 and 10). Based on limited data, a change in vessels did not affect tow swept area.

Insufficient information is available to rigorously evaluate the possible change in catch due to a reduction in tow distance, as time is confounded with tow distance. Table 7 provides a comparison obtained by differencing catches in a given season from 2-nm tows from catches of the same species in the same season, but in the subsequent year, from 1-nm tows. Only the target species were analyzed. Swept-area catches were compared with the expectation that the difference between catches for a given season and species should not diverge significantly from zero. Catches diverged significantly in three of eight cases (Wilcoxin signed-rank test, $\alpha = 0.05$), more than chance would allow, but in one case the divergence is positive and, in the other two, the divergence is negative. Regardless of significance, the divergence is positive in three cases and negative in five, a distribution anticipated to occur

Figure 8. Mean tow time (h) at each target depth (m) sampled during all surveys. Solid lines represent the target tow times based on an assumed 3-knot speed and a tow distance currently set at 1 nm but, prior to May 2004, at 2 nm.

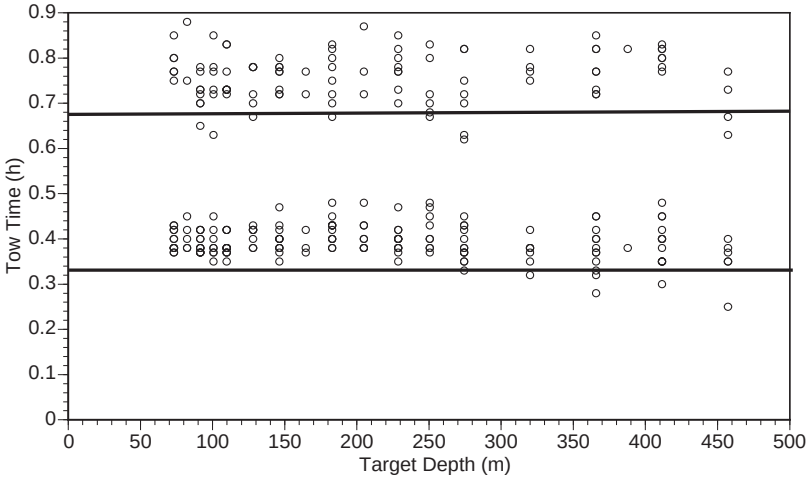

Figure 9. Mean swept area (km^2) for each survey and transect. Blue bars represent trips made on the *F/V Jason* & *Danielle* and black bars represent trips made on the *F/V Luke* & *Sarah*. Solid bars represent the Hudson Canyon transect and checkered bars represent the Baltimore Canyon transect. The horizontal black lines indicate Tukey's grouping where surveys that fall within the same Tukey's grouping are not significantly different at $\alpha = 0.05$.

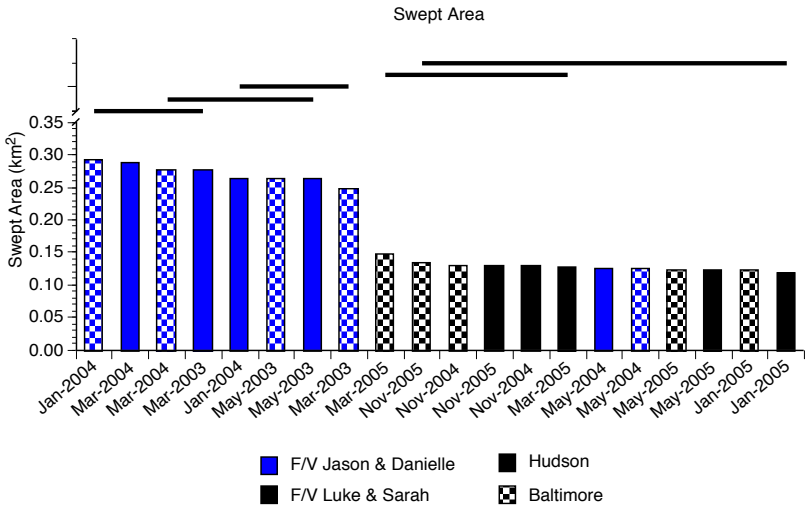

by chance under the expectation of an even split (Binomial test, $\alpha = 0.05$). The analysis does not support a change in catch per area swept in changing tow length from 2 nm to 1 nm.

Figure 10. Mean swept area (km^2) at each target depth (m) sampled during all surveys. The upper group are 2-nm tows. The lower group are 1-nm tows.

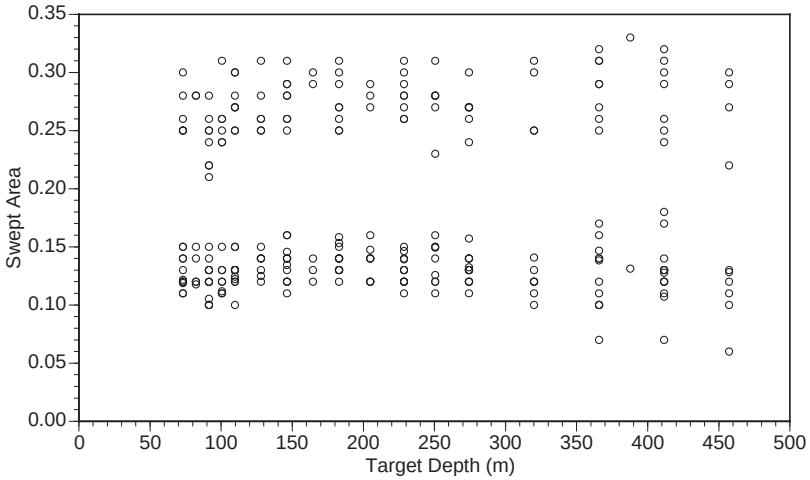

Table 7. Arithmetic and harmonic mean differences in swept-area catch between 1-nm and 2-nm surveys. Wilcoxon signed-rank tests evaluated the null hypothesis $H_\circ = 0$; that is, that no catch differences exist between 1-nm and 2-nm tows. All means are in kg.

Species	Arithmetic Mean Difference	Arithmetic Mean 2-nm Tows	Arithmetic Mean 1-nm Tows	Harmonic Mean Difference	Wilcoxin Signed-rank P-value	Sample Size
Black Sea Bass	8.8	83.4	74.6	4.3	0.0504	29
Loligo Squid	-131.3	484.7	616.0	101.4	0.2841	50
Monkfish	-85.8	201.8	287.7	5.5	0.0010	57
Offshore Hake	-86.5	474.1	560.5	54.6	0.8235	36
Scup	481.5	662.5	181.0	5.8	0.1475	26
Silver Hake	-1,748.9	325.4	2,074.3	-38.6	0.0001	49
Spiny Dogfish	-205.7	2,231.6	2,437.3	-16.8	0.1888	56
Summer Flounder	181.6	493.5	311.9	-87.8	0.5576	33

Depth, Depth Range, and Scope

A plot of average factor scores for Factor 5, upon which depth loaded (Figure 11) shows two strong outliers, the November, 2005, Baltimore and Hudson Canyon transects. The next three highest include the two November, 2004, transects and one from March, 2003 (Figure 12). A closer inspection of the depths on the Hudson and Baltimore Canyon transects for November, 2005, reveals that the observed depths were 9 m deeper on average then the target depths; thus, the residuals were high for that survey. *A posteriori* re-calibration revealed that the cause was a malfunction

in a *Vemco* minilogger*. Why November, 2004, falls somewhat outside of the range of other surveys is unclear. Other than as a result of sensor malfunctions, average depth has varied little over all survey-transects, as expected from the repeat-station sampling protocol. Average depths have varied less at the shallower stations, a fact not surprising given the steep slope at the deeper stations along the transects, particularly on the Baltimore Canyon transect (Figure 13).

Figure 11. PCA factor plot of Factor 5, describing the depth-standardized residual of average depth, versus Factor 6, describing average tow speed.

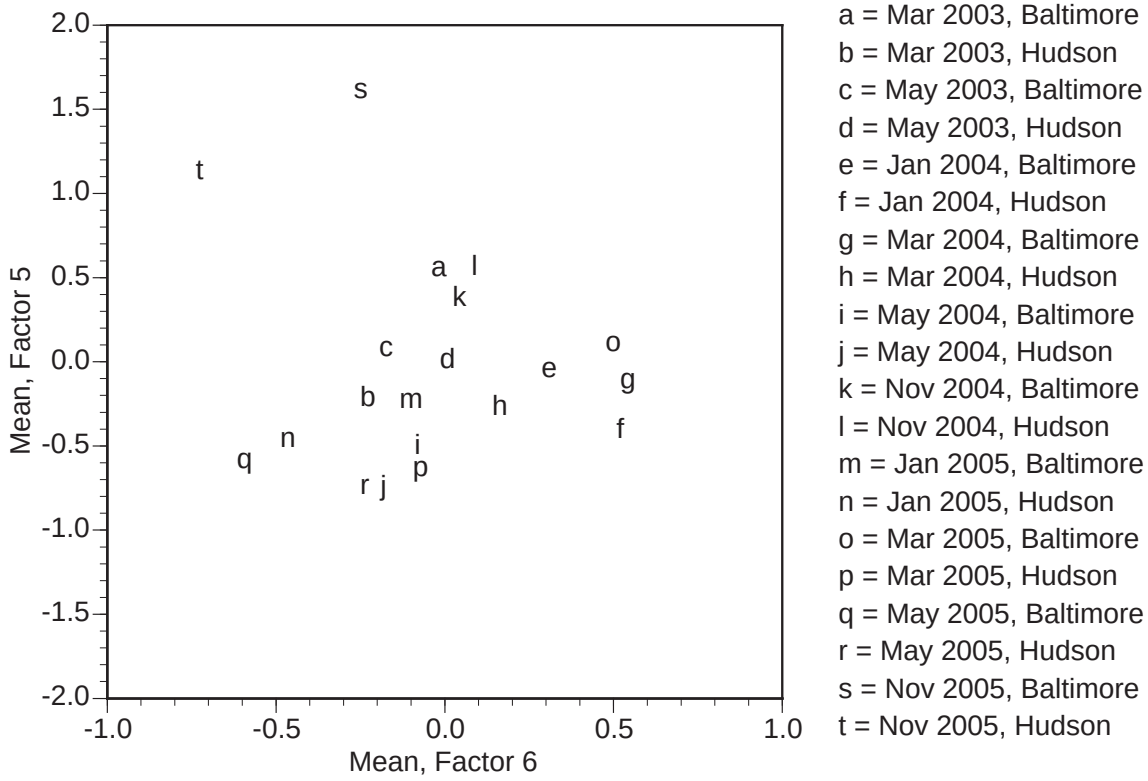

The depth-standardized residual of depth range loaded heavily on Factor 4. Significant differences existed among trips and transects (ANOVA, $P<0.0001$). Only four survey-transects diverged substantively from the remainder (Figure 14), however: the May, 2004, survey of the Hudson Canyon transect and three Baltimore Canyon transects, in May, 2003, in May, 2004, and in March, 2005. The depth range increased substantially with increasing depth (Figure 15) due to increasing variability in the alongslope topography at deeper depths. The set of depth ranges for any target depth also tended to diverge into two groups at deeper

* In subsequent surveys, redundant miniloggers have been deployed to reduce the likelihood of a repeat occurrence.

Figure 12. Depth-standardized residual of average depth for each survey and transect. Blue bars represent trips made on the *F/V Jason & Danielle* and black bars represent trips made on the *F/V Luke & Sarah*. Solid bars represent the Hudson Canyon transect and checkered bars represent the Baltimore Canyon transect. The horizontal black lines indicate Tukey's grouping where surveys that fall within the same Tukey's grouping are not significantly different at $\alpha = 0.05$.

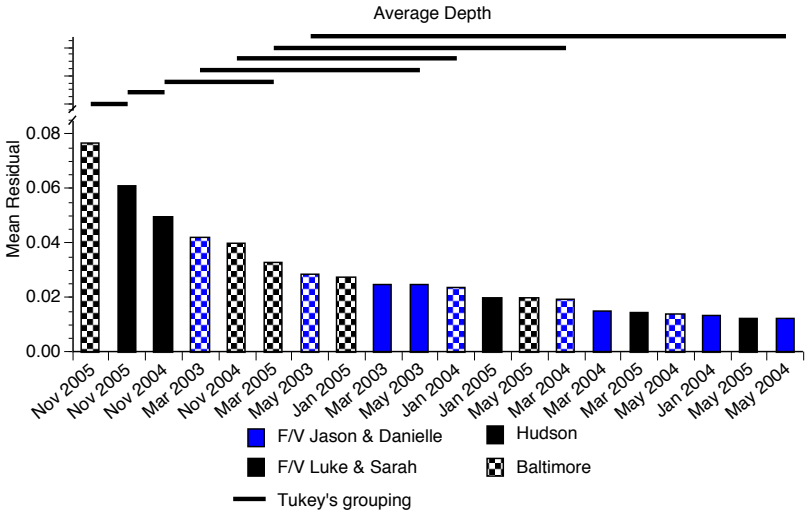

Figure 13. Comparison of average depth versus target depth (m). Target depths may have two data points from the same survey because data from both Hudson and Baltimore Canyon transects are included.

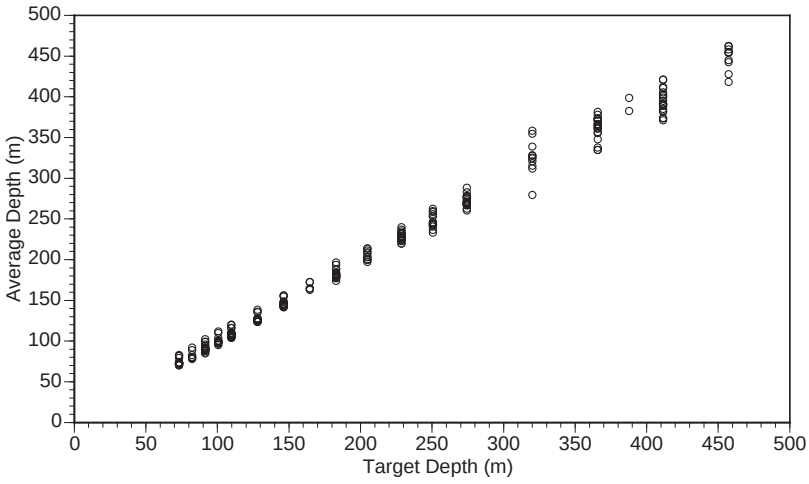

target depths, due to the increased topographic complexity on the Baltimore and Poor Man's Canyon transects relative to the Hudson and Alvin canyon transects. Not surprisingly, two of the three outlier survey-transects are Baltimore Canyon

transects (Figure 14). Nevertheless, overall, few substantial differences exist among the survey-transects (Figure 16). Both transects during the May, 2004, survey were outliers and this is likely due to the fact that the *Vemco* minilogger software malfunctioned during this survey and depth profiles from previous surveys were used to re-construct the May, 2004, depth profile (Figures 15 and 16).

Figure 14. Average factor scores for survey-transects for Factor 2, describing door spread, versus Factor 4, describing the depth-standardized residual of depth range.

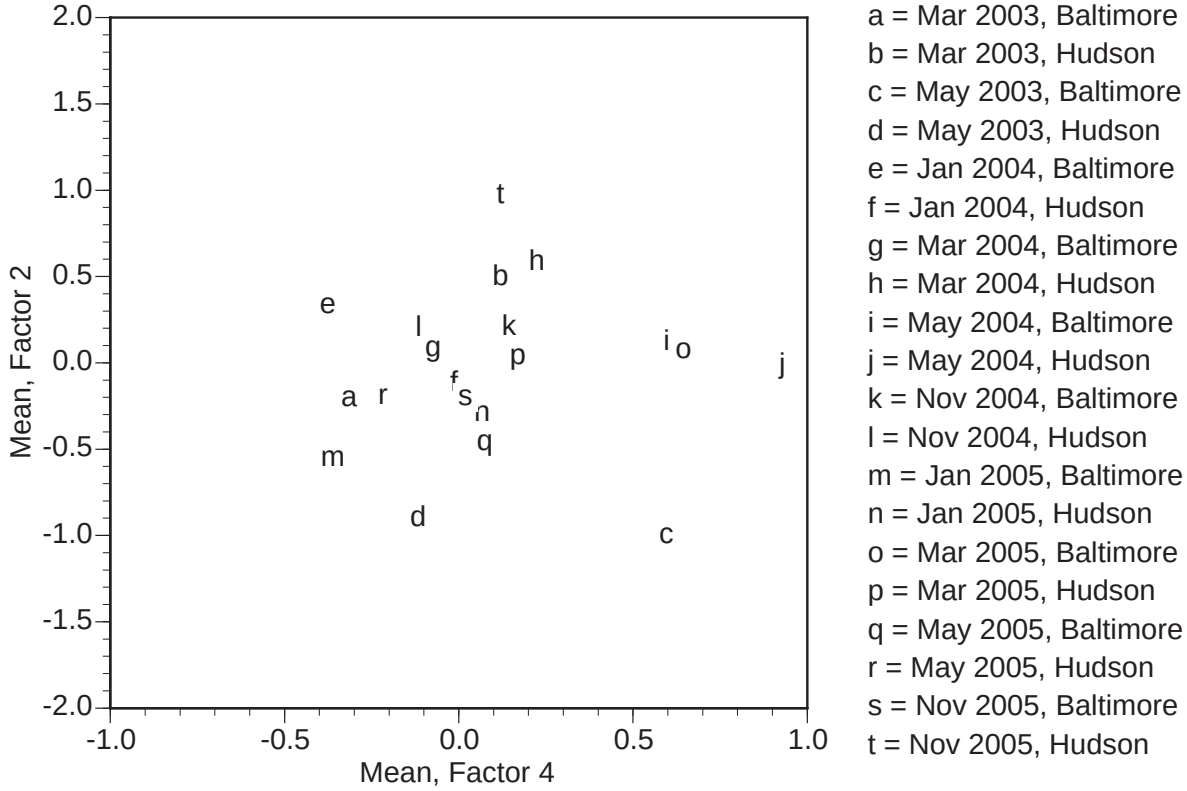

The depth-standardized residual for scope loads on Factor 3 (Figure 4). Significant differences among transects and surveys were observed (ANOVA, $P<0.0001$). Outliers included the two November, 2005, surveys with aberrant depth measurements, as previously explained, the two March, 2003, transects, and the November, 2004, Hudson Canyon transect (Figures 4 and 17). Scope values for March, 2003 were not used to generate the scope table (Tables 1 and 2) in May, 2004, as a consequence. Why March, 2003, varies from most other surveys is unclear, as retrospective discussion of the issue with vessel's personnel did not reveal any reason to believe that the net was not fishing properly. Very likely, the captain's records for this trip are less accurate. Nevertheless, the variance in scope at a given depth was relatively small across all surveys and transects (Figure 18).

Figure 15. Comparison of depth range versus target depth (m). Target depths may have two data points from the same survey because data from both Hudson and Baltimore Canyon transects are included.

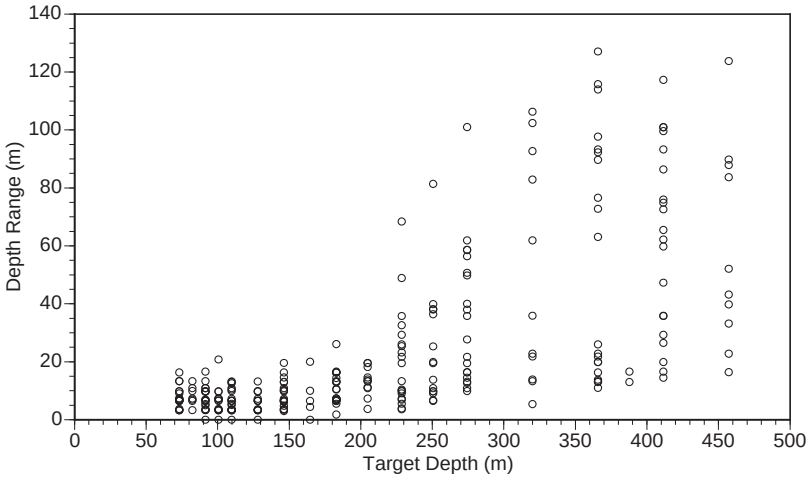

Figure 16. Depth-standardized residual of depth range for each survey and transect. Blue bars represent trips made on the *F/V Jason & Danielle* and black bars represent trips made on the *F/V Luke & Sarah*. Solid bars represent the Hudson Canyon transect and checkered bars represent the Baltimore Canyon transect. The horizontal black lines indicate Tukey's grouping where surveys that fall within the same Tukey's grouping are not significantly different at $\alpha = 0.05$.

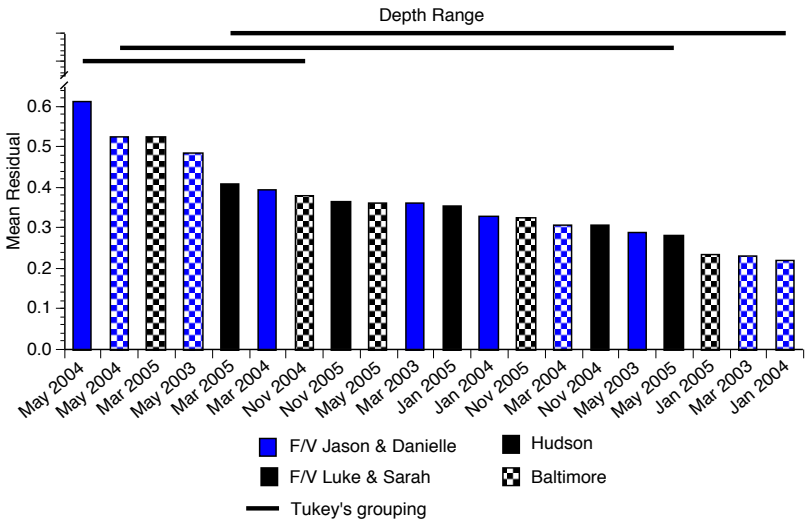

Tow Speed and Door Spread

Tow speed load principally on PCA Factor 6, although also contributing to

Figure 17. Average scope for each survey and transect. Blue bars represent trips made on the *F/V Jason* & *Danielle* and black bars represent trips made on the *F/V Luke* & *Sarah*. Solid bars represent the Hudson Canyon transect and checkered bars represent the Baltimore Canyon transect. The horizontal black lines indicate Tukey's grouping where surveys that fall within the same Tukey's grouping are not significantly different at $\alpha = 0.05$.

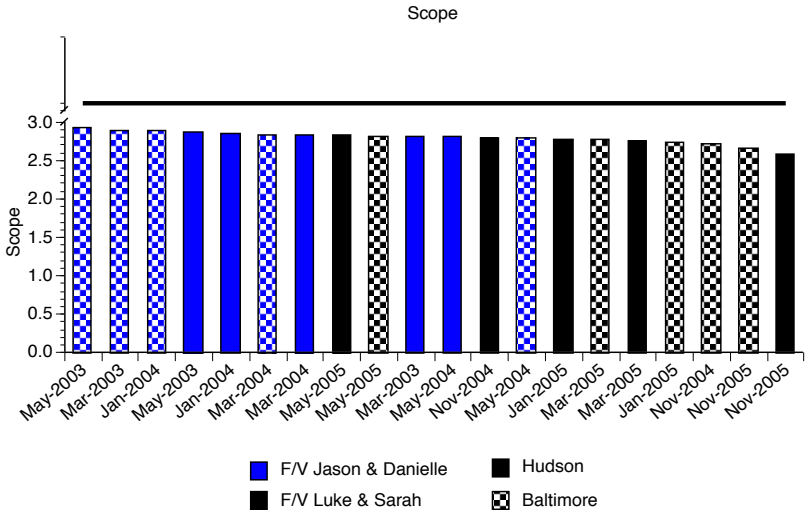

Figure 18. Comparison of scope versus target depth (m). Target depths may have two data points from the same survey because data from both Hudson and Baltimore Canyon transects are included.

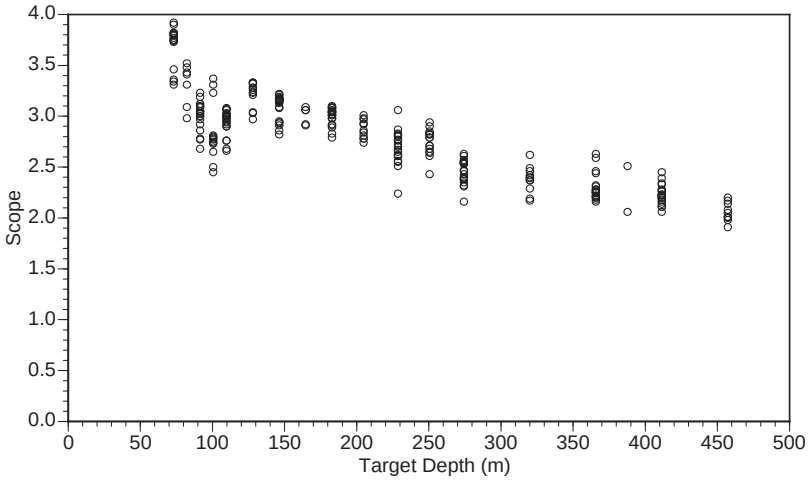

Factor 1 (Figure 11). Tow speed differed significantly among surveys and transects (ANOVA, $P<0.0001$). Mean speed per trip ranged from 4.72-5.43 km h^{-1} (Figure 19). Average tow speed tended to be higher during the January and March surveys

(5.08-5.19 km h^{-1}) versus the May and November surveys (4.81-4.97 km h^{-1}). The difference possibly originates in the need to compensate for increased wind and wave action during the winter. Nearly all outlier high-speed tows were from January and March surveys (Figures 19 and 20). Tow speeds recorded on the *F/V Luke & Sarah* appear to be slower on average than those recorded on the *F/V Jason & Danielle* (Figure 20). However, this differential is not a function of vessel performance differences but rather, can be explained by the interaction of the haulback procedure with the change in target tow distance. All 2-nm tows were performed on the *F/V Jason & Danielle*. Though the vessels try to maintain speed during haulback, a decrease in speed is necessary to compensate for added strain on the winches as the wire is reeled in. Because a time lag exists between initiation of the haulback procedure and the time that the gear leaves the bottom, the slower speeds during haulback reduce the average speed per tow. The slower speed during haulback has more impact on average speed during the tow as tow duration decreases, and thus average speed drops in 1-nm tows. This is the origin of the tendency for tow speed to load on Factor 1, with tow distance and tow time, as well as on its own unique factor.

Figure 19. Comparison of tow speed (km h^{-1}) versus target depth (m) from the January/March (Winter) surveys and the May/November (Fall/Spring) surveys. Target depths may have two data points from the same survey because data from both Hudson and Baltimore Canyon transects are included.

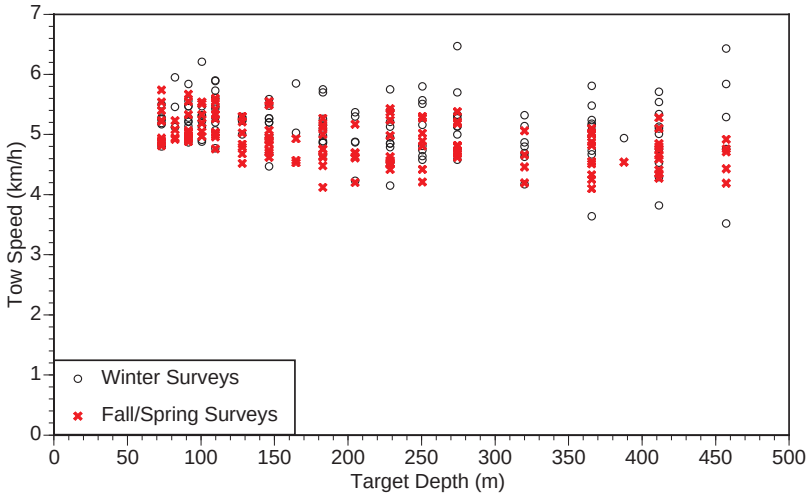

Door spread (m), the distance between the port and starboard doors measured by *Simrad* net mensuration equipment, were recorded manually on the bridge every 5 minutes. Door spread loaded on PCA Factor 2 (Figure 14). Mean door spread differed significantly among surveys and transects (ANOVA, $P<0.0001$) and ranged from 114.7-135.3 m with an overall mean of 124.0 m (Figures 21 and 22). Although

Figure 20. Mean tow speed (km h^{-1}) for each survey and transect. Blue bars represent trips made on the *F/V Jason & Danielle* and black bars represent trips made on the *F/V Luke & Sarah*. Solid bars represent the Hudson Canyon transect and checkered bars represent the Baltimore Canyon transect. The red line indicates the target value and the horizontal black lines indicate Tukey's grouping where surveys that fall within the same Tukey's grouping are not significantly different at $\alpha = 0.05$.

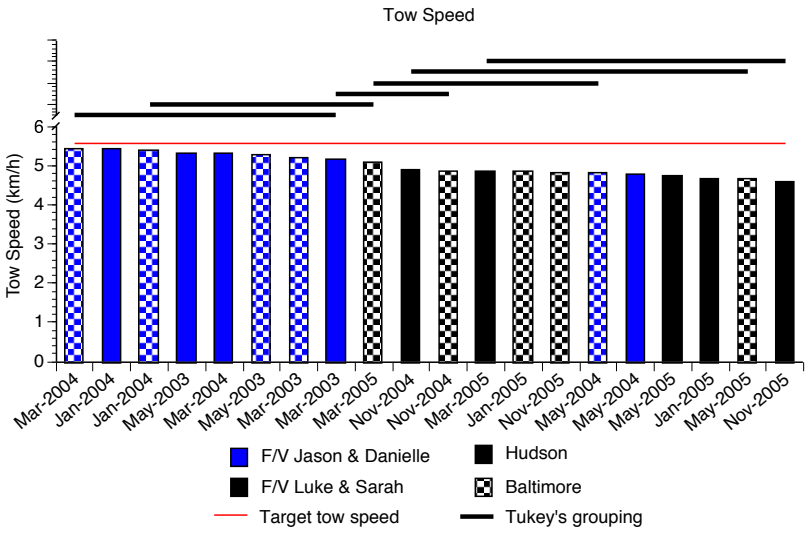

a Tukey's test revealed a complex array of groupings of survey-transects, the range in means differed by little more than 10% across all surveys and transects. Limited data suggest no difference between the two boats. Thus, door spread was very consistent within a survey, and diverged only moderately between surveys.

Comparison of Biomass Estimates

One of the most challenging aspects of a fixed+adaptive transect sampling design in a random, stratified world is how to incorporate the data into the stock assessment process. NMFS-NEFSC conducts a multispecies bottom trawl survey in March of every year. A number of commercially-important fish stocks, such as silver hake, are assessed based on this survey and so, the March component of the Supplemental Finfish Survey is scheduled to coincide with the spring component of the federal survey.

The NMFS survey is a stratified random survey with multiple stations taken per stratum. Three strata cover the depth range of the Supplemental Finfish Survey for any given transect[⊕]. The Supplemental Finfish Survey comprises a series of

[⊕] The Hudson Canyon transect runs through NMFS strata 1020, 1030, and 1040. The

Figure 21. Mean door spread for each survey and transect. Blue bars represent trips made on the *F/V Jason* & *Danielle* and black bars represent trips made on the *F/V Luke* & *Sarah*. Solid bars represent the Hudson Canyon transect and checkered bars represent the Baltimore Canyon transect. The horizontal black lines indicate Tukey's grouping where surveys that fall within the same Tukey's grouping are not significantly different at $\alpha = 0.05$.

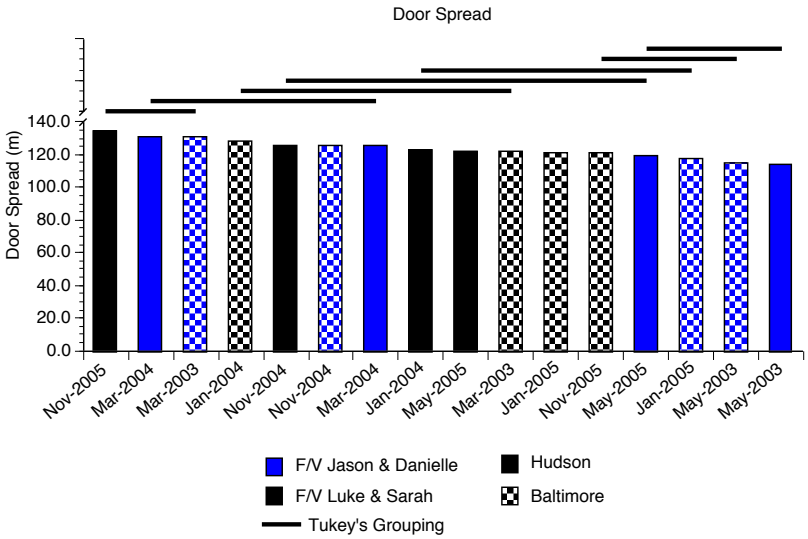

Figure 22. Mean door spread (m) at each target depth (m) sampled during all surveys. Target depths may have two data points from the same survey because data from both Hudson and Baltimore Canyon transects are included.

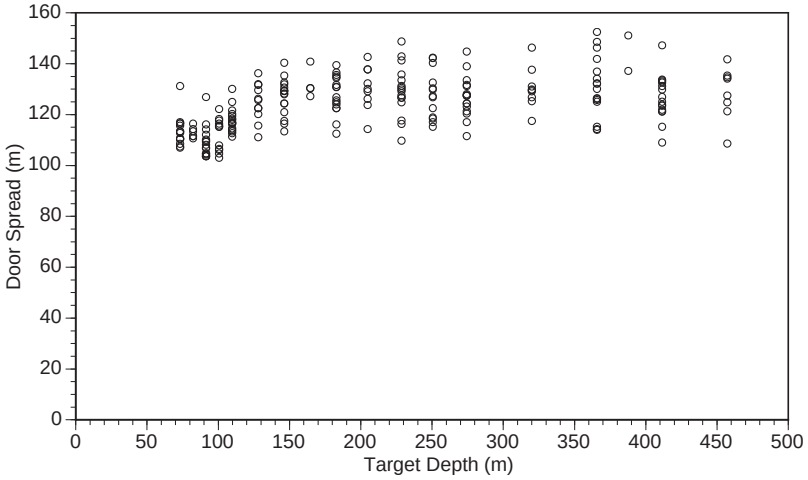

conterminous strata of sampling intensity *one* crossing the same depth gradient.

Baltimore Canyon transect runs through NMFS strata 1700, 1710, and 1720.

Comparison between the two requires mapping the smaller Supplemental Finfish Survey (SFS) strata onto the larger NMFS strata and to obtain an analagous catch value for comparison.

One approach to this mapping is as follows. For a given NMFS stratum, the average catch per swept area for any stratum j, $B_{NMFS-SWP_j}$ (in kg km^{-2}) is obtained by averaging the individual catches, i, within the strata standardized to tow swept area:

$$B_{NMFS-SWP_j} = \frac{\sum_{i=1}^{n_{NMFS_j}} C_{NMFS_{ij}}}{n_{NMFS_j}} \tag{20}$$

where $C_{NMFS_{ij}}$ is the swept-area biomass (in kg km^{-2}) at each station sampled within NMFS stratum j and n_{NMFS_j} is the total number of sampled stations. Total stratum biomass can then be obtained by multiplying by stratum area:

$$B_{T_{NMFS_j}} = B_{NMFS-SWP_j}\, SWT_{NMFS_j} \tag{21}$$

and domain biomass can be obtained by summing the n_j strata.

Comparison to the Supplemental Finfish Survey (SFS) can be accomplished by first recognizing that the supplemental survey is a conterminous sequence of strata of sampling intensity *one*. Stations within strata are averaged [e.g., equation (20)]; however, strata are added. The calculation is analogous to the use of Thiessen polygons to sum spatial data (McCullagh and Ross, 1980; Davis, 1986; Powell et al., 1995) or kriging (Johnsen, 2003; Petitgas and LaFont, 1997). Consequently, the first step is to identify each sampled target depth falling within a designated NMFS stratum and calculate the domain biomass value for that subset of samples by summing swath areas [equation (18)], with one modification. Some SFS strata may overlap the boundaries of the NMFS stratum, and so the swath area values for these strata must be prorated according to the degree of overlap. Let ξ be a weighting factor accounting for the mismatch of NMFS and SFS stratum boundaries. Then, from equation (18):

$$B_T = \sum_{i=1}^{\kappa} \xi_i B_{SWT_i} \tag{22}$$

where κ is the subset of SFS strata to be mapped onto the larger NMFS stratum. The average swept-area biomass for the SFS domain whose upslope and downslope extents are defined by the upslope and downslope boundaries of the NMFS stratum is then:

$$\widehat{B}_{SFS-SWP} = \frac{B_T}{\sum_{i=1}^{\kappa} \xi_i SWT_i}. \tag{23}$$

A comparison is generated using a set of data on silver hake provided by Larry Jacobson that were analyzed during the most recent silver hake assessment (NEFSC,

2006) (Table 8). NMFS stations were chosen to be near the SFS transect backbone and from the same month and year. SFS domain estimates are routinely higher for several reasons. First, the SFS survey gear is likely to have increased catchability in comparison to the NMFS survey gear (Powell et al., in press). Second, SFS station density is increased and, as will be shown in a later section, silver hake is routinely underestimated when sampling density is low.

Table 8. Silver hake biomass (kg km^{-2}) estimates based on catches from the March 2004 and 2005 NMFS-NEFSC random, stratified spring surveys and March 2004 and 2005 Supplemental Finfish Surveys. Calculations assumed a standard NMFS tow-door spread of 0.0238 km and a nominal tow distance of 3.8732 km.

Stratum Boundary (m)	NMFS Depth (m)	NMFS Mean Biomass (kg/km^2)	SFS Depth (m)	SFS Biomass (kg/km^2)
Hudson Canyon				
March 2004				
73-110	76	0.65	73, 89, 98, 104	662.4
111-183	114, 122	24.84	104, 125, 144, 165, 180	1,385.7
184-366	216	5.86	180, 226, 246, 267, 366	1,103.8
March 2005				
73-110	94, 97, 105	16.86	72, 90, 100, 109	837.3
111-183	120. 138	2.93	109, 128, 145, 182	1,546.3
184-366	289	305.05	182, 208, 228, 253, 271, 339, 366	11,128.1
Baltimore Canyon				
March 2004				
73-110	110	0.00	73, 91, 107	86.9
111-183	115, 116	10.74	107, 146, 163, 178	149.9
184-366	–	–	178, 200, 228, 233, 260, 327, 335	670.0
March 2005				
73-110	84	3.04	72, 81, 92, 99, 110	279.1
111-183	116, 135	4.90	110, 148, 188	448.2
184-366	355	12.58	188, 233, 243, 278, 355	5,640.3

Evaluation of Adaptive Station Value

Adaptive Station Analysis

The Supplemental Finfish Survey is unique in that it incorporates a fixed transect survey design with an adaptive sampling strategy. Given that the vessel costs are expensive, that certain depths are sampled during daylight or nighttime

hours, and that adaptive stations cannot be chosen until sampling of all fixed stations has been completed, it is important to evaluate whether or not the adaptive stations add substantially to the database.

The most commonly selected adaptive stations by sampling event were: 100.6, 250.6, and 320.0 m in January, 100.6 and 250.6 m in March, 100.6, 128.0, and 250.6 m in May, and 128.0, 204.8, and 250.6 m in November (Figure 23). From 2003 through 2005, 76 adaptive stations were sampled. Of those 76 stations, 65 (86%) were daytime stations whereas the other 11 (14%) were nighttime stations.

Figure 23. Sampling frequency of adaptive stations by survey month.

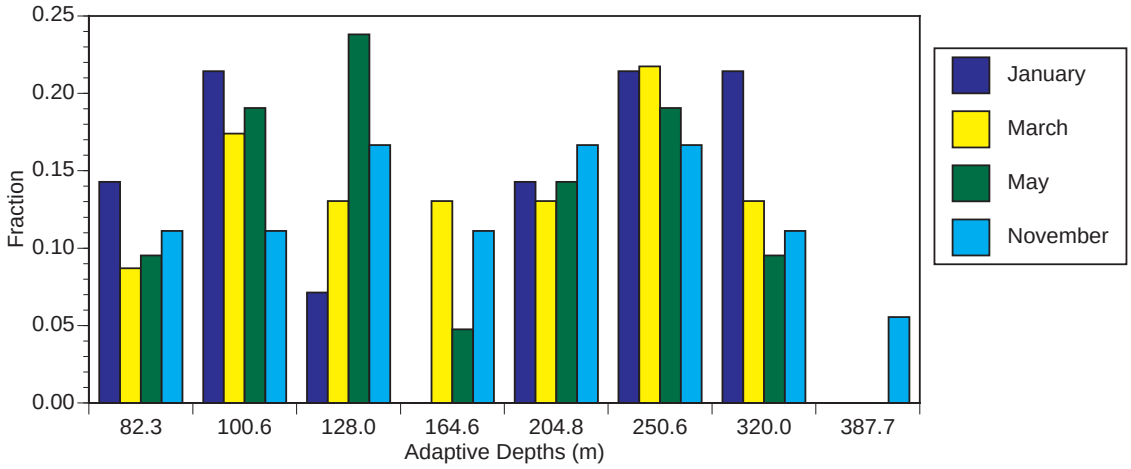

By sampling adaptive stations, an additional 2-15% more species were captured than if only fixed stations were sampled (Table 9). This is most likely a function of increased sample size (Farris and Lindgren, 1984; Bunt et al., 1984; Green and Young, 1993; Witman, et al., 2004).

The swath biomass was estimated based on the catches at fixed stations only and at fixed + adaptive stations and a ratio estimator was calculated. In order to estimate the biomass if only fixed stations had been sampled, the strata represented by adaptive stations must be collapsed onto the fixed-station strata. This is done by recognizing that neighboring fixed stations remain unaffected, but the swath area assigned to an adaptive station must be prorated to the fixed stations immediately upslope and downslope. The biomass represented by any fixed station, were only fixed stations sampled, B_{f_i}, is then:

$$B_{f_i} = \frac{\varepsilon_{i-1} B_{SWT_{i-1}}}{2} + B_{SWT_i} + \frac{\varepsilon_{i+1} B_{SWT_{i+1}}}{2} \qquad (24)$$

where $\varepsilon_{i-1} = 0$ for station 1, $\varepsilon_{i+1} = 0$ for station 19, and $\varepsilon = 0$ for all $i+1$ and $i-1$ that are fixed stations; $\varepsilon = 1$ for all other i. The biomass for any adaptive station

Table 9. The number of species caught on adaptive stations only, the percentage of species captured on adaptive stations only, and the total number of species caught on all stations.

Trip	Transect	# Species Caught on Adaptive Stations	Percent of Species Caught on Adaptive Stations	# Species Caught on All Stations
May 2003	Hudson	9	9.9	91
May 2003	Baltimore	3	3.4	88
Jan 2004	Hudson	4	6.2	65
Mar 2004	Hudson	2	2.8	71
Mar 2004	Baltimore	9	14.5	62
Mar 2004	Poor Man's	1	1.9	52
May 2004	Hudson	4	5.3	75
Nov 2004	Hudson	4	4.9	81
Nov 2004	Baltimore	5	6.4	78
Jan 2005	Hudson	5	6.5	77
Jan 2005	Baltimore	6	9.1	66
Mar 2005	Hudson	6	8.0	75
Mar 2005	Baltimore	3	4.8	62
Mar 2005	Poor Man's	3	3.8	65
May 2005	Hudson	5	6.3	80
May 2005	Baltimore	7	10.9	64
Nov 2005	Hudson	6	7.6	79
Nov 2005	Baltimore	6	7.7	78

$B_{f_i} = 0$. The ratio estimator then is calculated as:

$$RE_{_B} = \frac{\sum_{i=1}^{n_s} B_{f_i}}{\sum_{i=1}^{n_s} B_{f_i} + \sum_{i=1}^{n_s} B_{SWT_i}} \tag{25}$$

where, $RE_{_B}$ is the biomass ratio estimator. If no information is gained from sampling the adaptive stations, the expectation is that $RE_{_B} = 0.5$. When $RE_{_B} > 0.5$, the biomass estimated from fixed stations is higher than the biomass estimated from all, both the fixed and adaptive, stations. In other words, had sampling occurred only on fixed stations, biomass would have been overestimated. Conversely, if $RE_{_B} < 0.5$, an underestimate of biomass has occurred if sampling was restricted to the fixed stations only.

A summary of the results of this analysis for the biomass of all species, targeted and non-targeted, is displayed in Tables 10 and 11. The ratio estimator falls below 0.5 more often than expected by chance for many species. Thus, on average, reliance only on fixed stations frequently underestimates biomass. Binomial tests (Conover, 1980) were conducted for each species to see if biomass was underestimated or overestimated more often than expected by chance. The expectation is that values should diverge from 0.5 in either direction with equivalent likelihood. Of the target

species, the distribution of ratio estimators for silver hake, monkfish, and *Loligo* squid diverged significantly from that expected by chance ($P<0.1$); in each case, values falling below 0.5 occurred more frequently. Of the herrings, mackerels, and hakes, biomass estimates for Atlantic mackerel, red hake, spotted hake, silver hake and longfin hake diverged more often then expected by chance ($P<0.1$). The distribution of ratio estimator values diverged significantly from chance for a variety of other fishes and invertebrates. These included fourspot flounder, *Illex* and *Loligo* squid, buckler dory, deepbody boarfish, monkfish, tilefish, and chain dogfish, among others identified in Tables 10 and 11.

Additionally, extreme overestimates or underestimations, defined as ratio estimators <0.4 and >0.6, occurred frequently, often 20-25% of the time (Table 12). In other words, when the biomass estimate from fixed stations alone differs from the estimate based on fixed + adaptive stations, this differential is often large. Commonly, the likelihood of an extreme overestimate or underestimate is not randomly distributed. Extreme underestimates occur more frequently (Table 12), and often significantly so (Tables 10 and 11). Specifically in the case of the target species, extreme underestimates for silver hake, summer flounder, *Loligo* squid, and black sea bass occurred more frequently than overestimates and this difference exceeded that expected by chance (Binomial Test, $P<0.1$). In seven of nine cases, the number of extreme underestimates exceeded the number of extreme overestimates, also an unlikely occurrence ($P < 0.05$). Nontarget species also frequently had extreme discrepancies when values obtained from the fixed stations were compared to those obtained after including the adaptive stations and the distribution of these extremes often was also significantly biased (Tables 10 and 11).

Table 12. The number of trials in which extreme (<0.4 or >0.6) values of the ratio estimator occurred for each target species.

Species	Number of Trials <0.4	Number of Trials >0.6	Total Number of Trials
Black Sea Bass	4	0	18
Loligo Squid	4	0	18
Monkfish	1	0	18
Offshore Hake	1	0	18
Scup	3	1	16
Silver Hake	4	0	18
Female Spiny Dogfish	1	1	16
Male Spiny Dogfish	1	0	16
Summer Flounder	2	0	18

The comparison defined by equation (24) is potentially biased by the 175-fm

Table 10. The mean, standard deviation, and variance-to-mean ratio of the biomass ratio estimator RE_B for species sampled during 2003-2005 Supplemental Finfish Surveys. Binomial tests were conducted to evaluate the probability of observing a ratio greater than or less than 0.5 more often then expected by chance, the probability of observing an extreme ratio <0.4 or >0.6 more often then expected by chance, the probability that low ratios are associated with high catches more often then expected by chance, and the probability that high ratios are associated with high catches more often then expected by chance. Significance levels are as follows: *, P=0.1; **, P=0.05; ***, P=0.025; ****, P=0.02; *****, P=0.01; ******, P=0.005; *******, P=0.001; ********, P=0.0005; *********, P=0.0001. τ indicates a target species.

Species	Mean	Standard Deviation	Variance/ Mean	Ratio <0.5 vs. >0.5	Extreme Ratio <0.4 vs. >0.6	Low Ratio, High Catch	High Ratio, High Catch
Alewife	0.4955	0.0780	0.0123				
Atlantic Mackerel	0.3858	0.1742	0.0787	*	*****		
Atlantic Herring	0.4305	0.1674	0.0651		**	*	
Hickory Shad	0.4233	0.1896	0.0850				
Red Hake	0.4758	0.0919	0.0178	**			
White Hake	0.4246	0.1749	0.0721		*		
Offshore Hake$^{\tau}$	0.4955	0.0457	0.0042				
Silver Hake$^{\tau}$	0.4445	0.0557	0.0070	********	***		
Spotted Hake	0.4568	0.0392	0.0034	********			
Longfin Hake	0.5437	0.0503	0.0047	******	**	********	**
Monkfish$^{\tau}$	0.4750	0.0404	0.0034	*			
Fourspot Flounder	0.4595	0.0362	0.0028	********			
Gulfstream Flounder	0.4160	0.1385	0.0461		******		
Summer Flounder$^{\tau}$	0.4687	0.0582	0.0072		*		
Witch Flounder	0.4874	0.0496	0.0051				
Illex Squid	0.4484	0.0846	0.0159	**	**		*
Loligo Squid$^{\tau}$	0.4644	0.0790	0.0134	*****	***		
Batfish, Uncl.	0.5064	0.1018	0.0205	*			
Beardfish	0.4019	0.1985	0.0981		**		
Blackbelly Rosefish	0.4679	0.0743	0.0118		**		
Black Sea Bass$^{\tau}$	0.4686	0.0973	0.0202		***		
Bluefish	0.4731	0.0764	0.0123		*		
Buckler Dory	0.3526	0.2009	0.1144	**	******		
Butterfish	0.4636	0.0906	0.0177		***		
Deepbody Boarfish	0.0007	0.0021	0.0068	*******	*******	**	
Scup$^{\tau}$	0.4542	0.1608	0.0569				
Streamer Bass	0.3520	0.2232	0.1416		**	*	
Tilefish	0.4535	0.0810	0.0145	*	*		

adaptive station. This station in unique is having an upslope fixed station sampled

Table 11. Continuation of Table 10. See Table 10 for details.

Species	Mean	Standard Deviation	Variance/ Mean	Ratio <0.5 vs. >0.5	Extreme Ratio <0.4 vs. >0.6	Low Ratio, High Catch	High Ratio, High Catch
Armored Sea Robin	0.4735	0.0883	0.0165		**		
Northern Sea Robin	0.4698	0.0797	0.0135		*		
Striped Sea Robin	0.4312	0.1662	0.0640		*		*
Chain Dogfish	0.4482	0.0539	0.0065	********	**		
Smooth Dogfish	0.4528	0.1508	0.0502		*		
Male Spiny Dogfish[7]	0.4805	0.0570	0.0068				
Female Spiny Dogfish[7]	0.5013	0.0673	0.0090				
Atlantic Torpedo Ray	0.4558	0.2328	0.1189				**
Barndoor Skate	0.5185	0.0545	0.0057				
Clearnose Skate	0.4169	0.2510	0.1511				
Little Skate	0.4740	0.0407	0.0035	**		*	
Rosette Skate	0.4231	0.1582	0.0592		****		
Smooth Skate	0.5178	0.1215	0.0285		*	*****	
American Lobster	0.4887	0.0657	0.0088		*		
Anemone Uncl.	0.5274	0.0926	0.0163		*		
Bathyal Swimming Crab	0.2904	0.2271	0.1776	**	****		
Crab Uncl.	0.3727	0.2280	0.1395		*		
Deepsea Red Crab	0.4957	0.0280	0.0016				
Galatheid, Uncl.	0.4788	0.0997	0.0208				
Hermit Crab Uncl.	0.4332	0.2201	0.1118				
Jonah Crab	0.4785	0.0308	0.0020	**			
Rock Crab	0.4479	0.1457	0.0474				
Sea Potato	0.5372	0.0867	0.0140	*	*		
Sea Scallop	0.5436	0.0916	0.0154	**	*		
Sea Star	0.4116	0.1761	0.0753		****		
Shrimp Uncl.	0.4528	0.1231	0.0334				
Spider Crab, Uncl.	0.5151	0.0678	0.0089	*			
Conger Eel	0.3641	0.2182	0.1308		*****		
Fawn Cusk Eel	0.2481	0.2889	0.3364		*	**	
Slender Snipe Eel	0.4580	0.1584	0.0548			******	*
Marlinspike	0.4670	0.1417	0.0430				
Longnose Grenadier	0.4040	0.1678	0.0697		***	***	*
Longnose Greeneye	0.5342	0.0523	0.0051	**		*	
Shortnose Greeneye	0.4926	0.2066	0.0866				

during daylight hours and a downslope fixed station sampled during nighttime hours. The 175-fm station is a nighttime station. Removal of this station from the dataset did not substantially influence the outcome of analyses yielding Tables

10, 11, and 12, however. Consequently, inclusion of the unique 175-fm adaptive station was not consequential in establishing the observed bias in the frequency of underestimation of biomass based on the fixed stations only.

To ensure that extremely high or low ratio estimators were not a function of high catches (> median catch), binomial tests evaluated whether the number of extreme low ratios or high ratios, respectively, and high catches co-occurred more often than expected by chance (right-hand two columns, Tables 10 and 11). Low ratios and high catches occurred together more often than expected by chance for a few nontarget species. Examples include Atlantic herring, longfin hake, deepbody boarfish, little skate, and smooth skate (Binomial Test, $P<0.1$). High extreme values of the ratio estimator and high catches co-occurred together more often than expected by chance as well for a few nontarget species. Examples include Atlantic torpedo ray, *Illex* squid, and striped sea robin (Binomial Test, $P<0.1$). However, for most of the species, including all target species, extreme values of the ratio estimator were not explained by a biased association with high or low catches (Tables 10 and 11).

An abundance-based ratio estimator, RE_A, was calculated per the model adopted by equation (24). This analysis was limited perforce to that subset of species for which lengths were obtained. Reliance on fixed stations resulted frequently in underestimating abundance, as observed for biomass (Table 13). For species of all sizes, underestimates occurred for *Illex* squid, monkfish, scup, silver hake, and female spiny dogfish. Extreme overestimates or underestimates, defined by ratio estimator values <0.4 and >0.6, also occurred frequently and this distribution was also biased favoring extreme underestimates for a number of species, including: black sea bass, *Illex* squid, *Loligo* squid, rosette skate, silver hake, smooth skate, and summer flounder (Binomial Test, $P<0.1$) (Table 13).

As examples, we also evaluated a few size classes for selected species: *Loligo* squid, spiny dogfish, and summer flounder. Biases occurred in size classes frequently, even when the entire species' abundance estimate was unbiased, and extreme values of the ratio estimator were also more common and often strongly biased. For *Loligo* squid, for example, fixed stations provided sufficient data for estimating abundance for the 0-10 cm size class but, for the 10+ cm size class, abundances tended to be underestimated more often than expected by chance (Binomial Test, $P<0.1$). For male spiny dogfish, fixed stations underestimated the number of pups (0-35 cm size class) and estimates for the 35-70 cm and 70-85 cm size classes tended to produce extremes in the ratio estimator with underestimates predominant (Table 13). Summer flounder exhibits a similar trend in that the 0-35 cm size class was underestimated based on fixed stations only more frequently than expected by chance and the frequency of extreme underestimates was noteworthy.

Table 13. The mean, standard deviation, and variance-to-mean ratio of the abundance ratio estimator for species sampled during 2003-2005 Supplemental Finfish Surveys. Binomial tests were conducted to evaluate the probability of observing a ratio greater than or less than 0.5 more often then expected by chance and the probability of observing an extreme ratio <0.4 or >0.6 more often then expected by chance. Significance levels are as follows: *, P=0.1; **, P=0.05; ***, P=0.025; ****, P=0.02; *****, P=0.01; ******, P=0.005; *******, P=0.001; ********, P=0.0005; *********, P=0.0001. τ indicates a target species. M, male; F, female.

Species	Size	Mean	Standard Deviation	Variance/ Mean	Ratio <0.5 vs. >0.5	Extreme Ratio <0.4 vs. >0.6
American Lobster	all sizes	0.4898	0.0637	0.0083		
Barndoor Skate	all sizes	0.5105	0.0634	0.0079		
Black Sea Bass	all sizes	0.4264	0.1612	0.0609		*****
Bluefish	all sizes	0.4851	0.0602	0.0075		
Clearnose Skate	all sizes	0.4119	0.2487	0.1501		
Illex Squid	all sizes	0.4298	0.1289	0.0387	*	**
Loligo Squid	all sizes	0.4591	0.1144	0.0285		**
Loligo Squid	0 to 10 cm	0.4794	0.0930	0.0180		
Loligo Squid	10 to 54 cm	0.4397	0.1261	0.0362	*	****
Monkfish	all sizes	0.4751	0.0378	0.0030	**	
Offshore Hake	all sizes	0.4762	0.1009	0.0214		
Rosette Skate	all sizes	0.4092	0.1634	0.0652		******
Scup	all sizes	0.4406	0.1987	0.0896	*	
Silver Hake	all sizes	0.4354	0.0949	0.0207	******	****
Smooth Skate	all sizes	0.5229	0.0925	0.0164		*
Spiny Dogfish-M	all sizes	0.4674	0.1164	0.0290		
Spiny Dogfish-M	0 to 35 cm	0.4548	0.1753	0.0676	*	
Spiny Dogfish-M	35 to 70 cm	0.4612	0.0976	0.0206		*
Spiny Dogfish-M	70 to 90 cm	0.4760	0.0934	0.0183		
Spiny Dogfish-F	all sizes	0.5053	0.1342	0.0356	*	
Spiny Dogfish-F	0 to 35 cm	0.4703	0.1867	0.0741		
Spiny Dogfish-F	35 to 70 cm	0.5201	0.0987	0.0187		
Spiny Dogfish-F	70 to 90 cm	0.4872	0.1581	0.0513		
Spiny Dogfish-F	90 to 98 cm	0.4488	0.2148	0.1028		
Summer Flounder	all sizes	0.4635	0.0770	0.0128		**
Summer Flounder	0 to 35 cm	0.4358	0.1487	0.0507	*	***
Summer Flounder	35 to 80 cm	0.4626	0.0766	0.0127		**

The tendency for abundance or biomass estimates based on fixed stations only to underestimate abundance or biomass, and to generate extreme underestimates more commonly than extreme overestimates, might be thought to be due to the increased likelihood that the center of the patch falls on an adaptive station. After all, adaptive stations are chosen specifically to determine if a biomass high identified by the fixed stations is properly located and the patch adequately resolved. Thus, adaptive stations might have a high chance of falling more precisely in the center

of a patch than the fixed stations. Although one cannot rigorously evaluate this likelilhood, without conducting an even more intense survey (e.g., Elliott, 1977), an approximation can be obtained by estimating the likelihood of the occurrence of species' distributional modes on fixed and adaptive stations.

We first estimate the chance that a mode is located on an adaptive station. Because some distributions are bimodal, occasionally more than one mode occurs for a species on a transect. We treat each as an independent occurrence. The expectation, on the Hudson Canyon transect, is that a mode would occur on an adaptive station with a frequency of 0.333. The value on the Baltimore Canyon transect is slightly lower, at 0.308. Rarely do adaptive stations occur more or less frequently as modes than expected by chance (Table 14).

Table 14. A tally of the frequency in which patch modes occur on adaptive stations or fixed stations.

Species	Transect	Adaptive Station	Fixed Station
Black Sea Bass	Hudson	2	11
	Baltimore	3	7
Loligo Squid	Hudson	5	11
	Baltimore	2	10
Monkfish	Hudson	8	10
	Baltimore	4	14
Offshore Hake	Hudson	6	7
	Baltimore	2	9
Scup	Hudson	2	7
	Baltimore	2	6
Silver Hake	Hudson	5	12
	Baltimore	5	9
Female Spiny Dogfish	Hudson	8	6
	Baltimore	0	12
Male Spiny Dogfish	Hudson	6	8
	Baltimore	4	8
Summer Flounder	Hudson	2	10
	Baltimore	3	7

The frequency of bimodal distributions is noteworthy, and sometimes, both modes fall on adaptive stations. In cases where bimodal distributions occur, do one or both modes occur on adaptive stations more frequently than expected by chance? Three combinations are possible for bimodal distributions: fixed-fixed, fixed-adaptive, and adaptive-adaptive modes. For the Hudson Canyon transect, the expected probability, if species' modes were distributed among station types in these three ways by chance, is 0.439, 0.245, and 0.71, recognizing that the second mode cannot co-occur with the first (choice without replacement). For

the Baltimore Canyon transect, the values are somewhat different: 0.462, 0.461, and 0.77, respectively. The three possible combinations of modes occur, in most cases, in the proportions expected by chance (Table 15). Thus, the tendency for biomass (and abundance) to be underestimated based on the fixed stations only is not simply explained by improved identification of the highest biomass or abundance in the patch by the adaptive stations. The explanation must reside in a more subtle interplay between patch shape and location. It is noteworthy, for example, that cases where the highest catch occurred at a fixed station, such as silver hake on the Hudson Canyon transect in November, 2005, nevertheless yielded ratio estimator values well under 0.5; 0.42 in the aforementioned case (Figure 24).

Figure 24. Swath-area biomass for silver hake along the Hudson canyon transect in November, 2005. Tow numbers indicate the sampling sequence during the cruise. Tows are ordered shallowest to deepest along the x-axis according to the depth profile shown as the solid line.

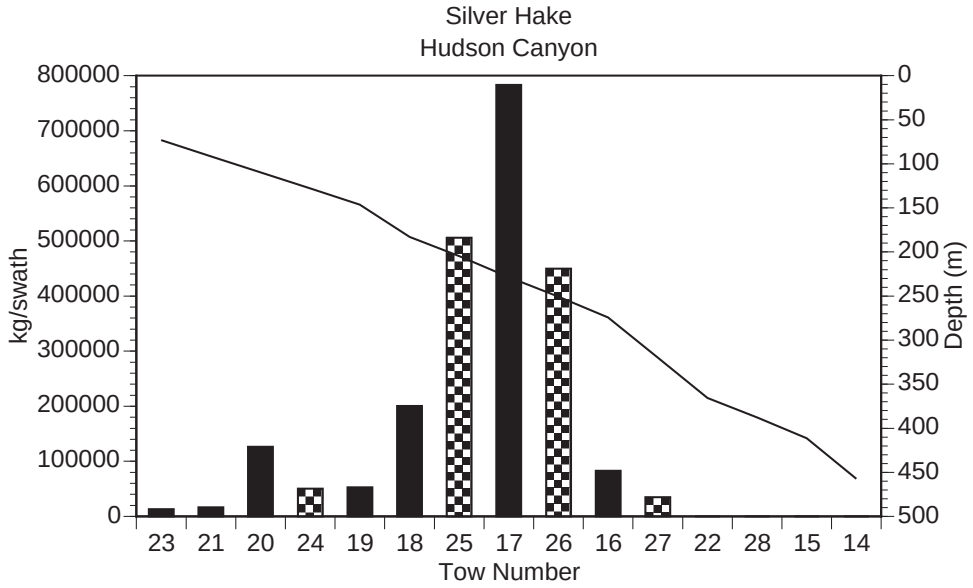

Modeling of Adaptive Sampling Protocol

Survey adequacy can be evaluated in terms of precision and accuracy. Typically, coefficients of variation are used to evaluate precision. Station density within a stratum normally is judged adequate when coefficients of variation are relatively low. Good precision does not necessarily imply accuracy, however. Accuracy is best evaluated by increasing sample number (Findlay, 1982; Green and Young, 1993; Hjellvik et al., 2002). If an increased sample number returns a similar biomass estimate for a stratum, then the original sample density is likely to provide an adequate estimate of biomass. Typically, sampling must resolve significant patch dynamics of the evaluated species, as they exist within the domain or stratum (e.g. from a

Table 15. A tally of the frequency in which bimodal patch modes occur as adaptive-adaptive, adaptive-fixed, and fixed-fixed pairs.

Species	Transect	Adaptive-Adaptive	Fixed-Adaptive	Fixed-Fixed
Black Sea Bass	Hudson	0	0	4
	Baltimore	0	1	0
Loligo Squid	Hudson	1	3	3
	Baltimore	0	2	1
Monkfish	Hudson	3	2	4
	Baltimore	1	2	6
Offshore Hake	Hudson	2	1	1
	Baltimore	0	0	2
Scup	Hudson	0	1	0
	Baltimore	0	0	0
Silver Hake	Hudson	1	3	4
	Baltimore	0	2	3
Female Spiny Dogfish	Hudson	2	4	0
	Baltimore	0	0	4
Male Spiny Dogfish	Hudson	0	5	1
	Baltimore	1	1	2
Summer Flounder	Hudson	0	0	3
	Baltimore	1	0	0

plethora of similar treatments: Clark and Evans, 1954; Elliott, 1977; Jumars et al., 1977; Findlay, 1982; Powell et al., 1987; Meyers et al., 1987; Green and Young, 1993; Peterson et al., 2001). The adaptive sampling protocol seeks to introduce increased sampling density during standard survey practice to evaluate survey accuracy 'on the fly', rather than *a posterior* (e.g., Vignaux, 1996) or through *a priori* evaluation of required sampling density (e.g., Green, 1989; Smith et al., 2003; Battista, 2003).

Analysis of abundance and biomass based on the fixed stations in comparison to the same measures obtained after the addition of the adaptive stations indicates that the sampling density of the fixed stations routinely results in inaccurate estimates of abundance and biomass. These inaccuracies are not random. Extreme discrepancies occur relatively often and underestimates occur significantly more often than overestimates. That is, not only do extreme inaccuracies occur frequently, but biases occur consistently. Silver hake is an exemplar of the latter case. However, these discrepancies are not explained by the consistent identification of the patch mode by the adaptive stations.

The question is: why do these biases exist? We investigate this question by means of a numerical model of a transect composed of 19 stations, ten fixed stations and 9 possible adaptive stations, one each between each pair of fixed stations. Initially, we allocate animals along this transect in the form of a single patch of varying dimensions, but defined shape. We establish a gradient in stratum

dimension typical of that found on the Hudson Canyon transect. On this transect, the swath area allocated to stations, equivalent to the stratum size, declines with depth. That is, stations are closer together geographically as depth increases (Figure 25). A regression of observed swath areas yields:

$$y = -0.91x + y_\circ \tag{26}$$

where y is the swath area, x is ranked depth with the shallowest station receiving a rank of 1, and $y_\circ$ is the swath area for theoretical station zero.

Figure 25. Relationship of patch size to transect length and swath area to station position for the theoretical Hudson Canyon transect defined by equation (26) (model patch, model station) and for the real Hudson Canyon transect defined by the distances between target depths (Hudson patch, Hudson station) (Table 1).

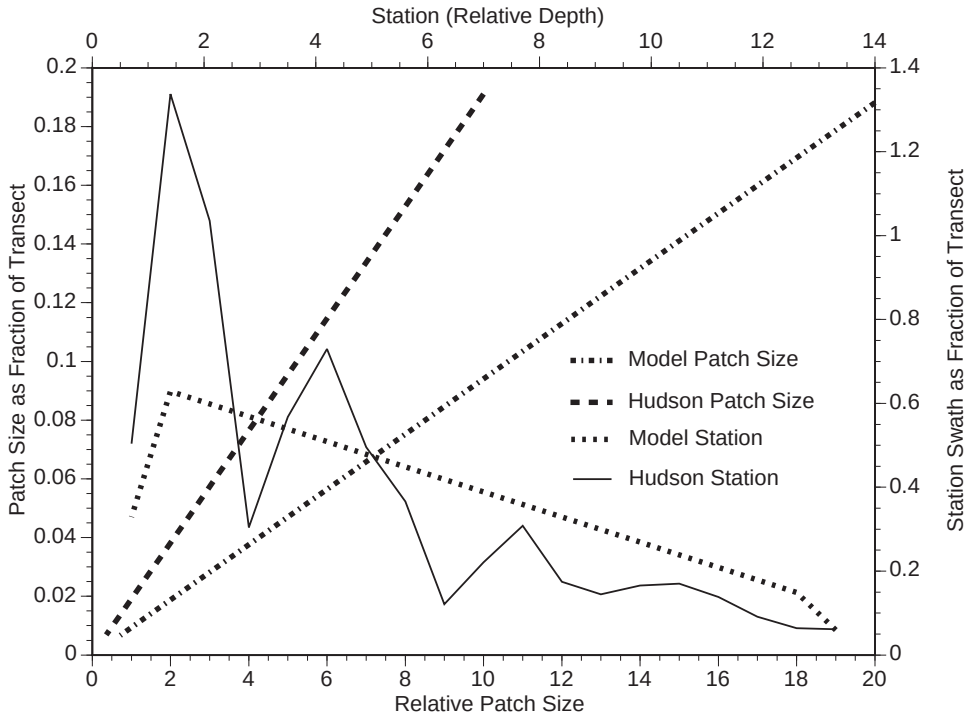

Figure 26 shows the results of a simulation in which the patch is defined by the zero-order equation:

$$\frac{d\,\mathcal{B}}{dd} = b \tag{27}$$

where $\mathcal{B}$ is biomass, the differential is the rate of change of biomass with distance, d, across the patch, and b is the unit concentration. If sampled in infinitely small segments, the patch would appear as a rectangular patch with sharp vertical boundaries (Figure 27). Equation (27) is integrated under the constraint that $b = 0$ for $d < d_d$ and $d > d_u$, where d_d identifies the downslope extent of the patch and d_u identifies the upslope extent of the patch. The linear dimension of the patch along

the transect is then: $L = d_u - d_d$ and, so, equation (27) is integrated from d_d to d_u and biomass is apportioned by the location of stratum boundaries within L. Specific rules are imposed when the patch extends upslope beyond station 1 or downslope below station 19, respectively: $L > L_f = d_{250} - d_d$ or $L > L_f = d_{40} - d_u$, where L_f is the portion of the patch falling within the survey domain. The simulated total catch for the transect, B_T [equation (18)], is computed using all 19 biomass values and also for the fixed stations only. For the latter evaluation, the swath areas are recomputed as in equation (24) based on the distances between the fixed stations only. The ratio estimator then is computed in the standard way [equation (25)]; thus, ratios above 0.5 indicate cases where the fixed stations analyzed alone yielded a biomass estimate above the value obtained from all samples.

Figure 26. Simulation of the Hudson Canyon transect using a depth-dependent gradient in swath area per station [equation (26)], a zero-order or rectangularly-shaped patch [equation (27)], 10 fixed (odd number) and nine adaptive (even number) stations, all sampled, and a series of patch sizes. Patch size is defined relative to the swath area for station 2 (Figure 25), the largest complete stratum sampled.

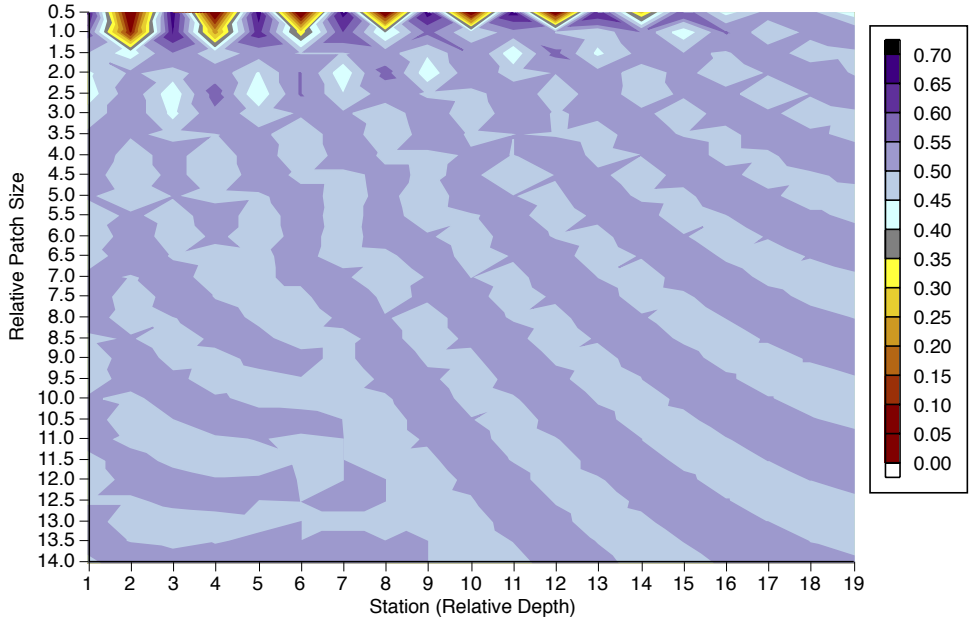

Figure 26 shows that extreme events occur when patch size is small relative to the dimensions of the stratum. When the patch is centered on an adaptive station, estimated transect biomass from the fixed stations severely underestimates true biomass. When the patch is centered on a fixed station, estimated transect biomass from the fixed station alone severely overestimates true biomass. The patch size necessary to generate an extreme event declines with depth because the swath area

Figure 27. Cartoon depiction of the zero-order patch [equation (27)], the first-order patch [equation (28)], and the second-order patch [equation (29)]. Note that the zero-order patch, if the patch boundaries do not coincide with the stratum boundaries, will appear as a dome-shaped patch when sampled by discrete stations.

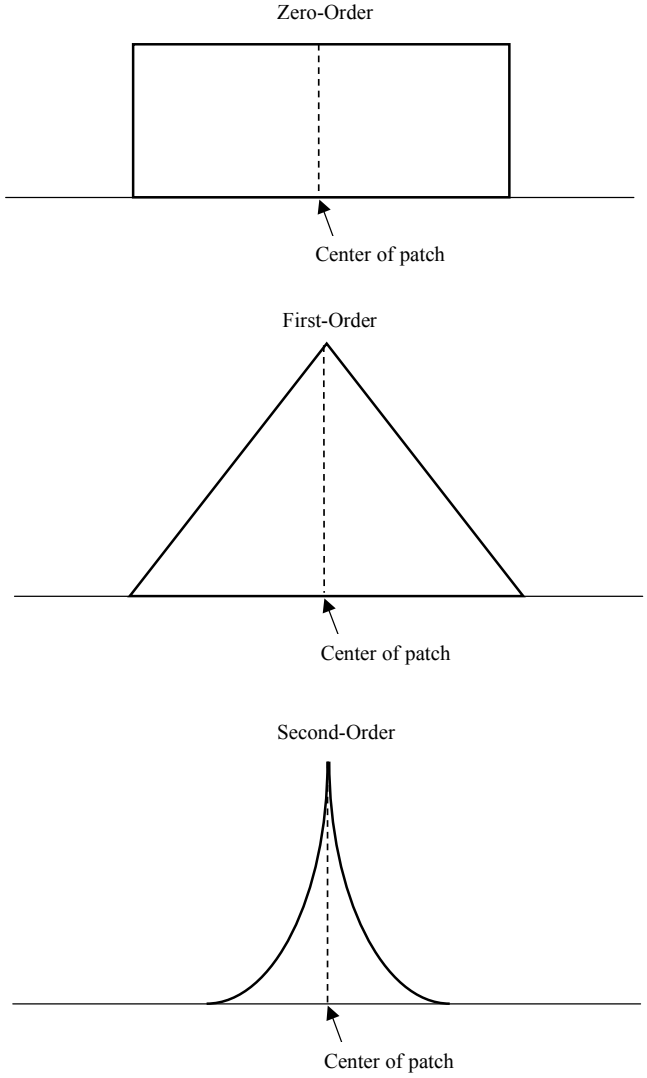

allocated to deeper strata (stations) declines with depth. Thus, extreme events are more likely to be caused by small, relative to stratum dimensions, patches centered on shallower stations. Larger patches routinely produce ratio estimator values of 0.45-0.55, and, in fact, most of these values are between 0.49 and 0.51. Thus larger patches are adequately estimated by the fixed stations, regardless of the location of the patch or its absolute dimensions.

The result is not substantively impacted by patch shape. Figures 28 and 29 show equivalent simulations with first-order and second-order patches defined,

respectively, by:

$$\frac{d\,\mathcal{B}}{dd} = bd \tag{28}$$

and

$$\frac{d\,\mathcal{B}}{dd} = bd^2\,. \tag{29}$$

(Figure 27). Note that, in practice, the patch shape rendered in Figure 27 is obtained by integrating equations (28) and (29) from the edge of the patch to its center and its reflection. Thus $L = L_1 + L_2$ and $L_2 = pc - d_u$ where pc is the patch center.

Note in comparing Figures 26, 28, and 29 that the more extreme the shape of the patch, the more extreme the ratio estimator values for a given patch size. Thus, the second-order patch generates extreme ratio estimators for relative patch sizes more than double the zero-order patch, and the probability of an extreme value carries into the deeper, smaller, strata, given the same patch size. Note also that the likelihood of a ratio estimator above or below 0.5 is determined in large measure by the likelihood that the center of the patch falls on the adaptive or the fixed station. Fish such as silver hake that are routinely underestimated from the fixed stations are not thereby readily explained, as no reason exists to expect that patch centers should routinely fall at adaptive station depths (see also Tables 14 and 15).

Many distributional patterns are bimodal, at least to some degree. Bimodal distributions increase the complexity of the dynamics of sampling, patch location, and patch size. With the exception of the case where one of the two patches is very small and centered on a fixed station, any scenario in which one or more of the patches is centered on an adaptive station will produce an underestimate of biomass from the fixed stations only (Figure 30). In some cases, these underestimates will be extreme, but rarely so. Normally, when both modes are centered on fixed stations, an overestimate, sometimes, but rarely, an extreme overestimate of biomass, will be obtained (Figure 31). Cases where one or both patches are near the boundaries of the transect can generate unusually severe patterns in which extreme estimates predominate, however. Figure 32, for example, shows a case where extreme underestimates created by a patch near the upslope transect boundary assures an underestimate of biomass for the transect domain, regardless of the location and geographic extent of the other patch. One narrow patch, centered on an adaptive station away from the transect boundary, also assures an underestimate of biomass for the transect domain, regardless of the location and geographic extent of the other patch (Figure 33). So, as the patch narrows relative to the scale of the stratum, the likelihood of an extreme estimate rises, but bimodality can convert a potential overestimate from a patch centered on a fixed station into a realized underestimate, particularly if the other patch is both narrow and centered on an adaptive station.

Figure 28. Simulation of the Hudson Canyon transect using a depth-dependent gradient in swath area per station [equation (26)], a first-order or triangularly-shaped patch [equation (28)], 10 fixed (odd number) and nine adaptive (even number) stations, all sampled, and a series of patch sizes. Patch size is defined relative to the swath area for station 2 (Figure 25).

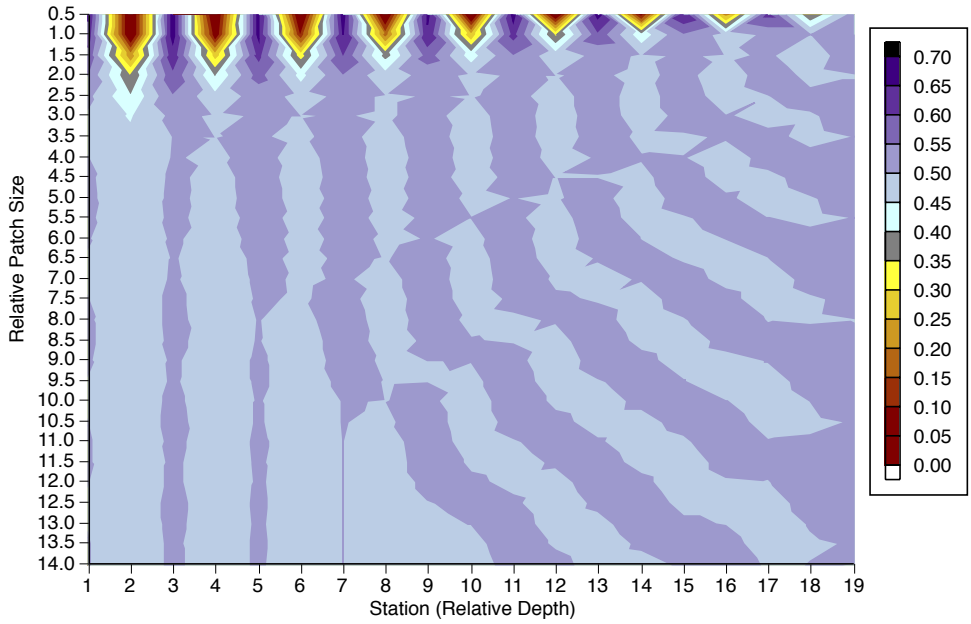

Now we know that overestimates of biomass from fixed stations alone are typically caused by one or more patches centered on fixed stations and extreme overestimates by relatively narrow patches so centered. Underestimates of biomass from fixed stations alone are typically caused by one or more patches centered on adaptive stations and extreme underestimates by relatively narrow patches so centered. This is not, however, the entire story. In Table 16, we summarize the ratio estimators for biomass for three target species: black sea bass, *Loligo* squid, and silver hake. The equivalent information for abundance is provided in Table 17. Black sea bass is characterized by a propensity towards large values of the ratio estimator. Six ratio estimator values fall outside of the range 0.45 to 0.55. Two of these five fall above 0.55. The other three fall below 0.45. *Loligo* squid is a species characterized by a greater frequency of ratio estimator values outside of the range 0.45 to 0.55 than black sea bass. Fully half of all survey transects yield ratio estimators of this kind. Yet, both extreme overestimates and extreme underestimates are common. Silver hake is a species with a high propensity for extreme ratio estimator values as well. However, in this case, all are underestimates.

Tables 16 and 17 assign five conditions to the extreme estimates for these three target species. A perusal of these tables reveals that a single mode on a fixed station invariably results in a ratio estimator above 0.55 when the value is outside of the

Figure 29. Simulation of the Hudson Canyon transect using a depth-dependent gradient in swath area per station [equation (26)], a second-order or hyperbolic-shaped patch [equation (29)], 10 fixed (odd number) and nine adaptive (even number) stations, all sampled, and a series of patch sizes. Patch size is defined relative to the swath area for station 2 (Figure 25).

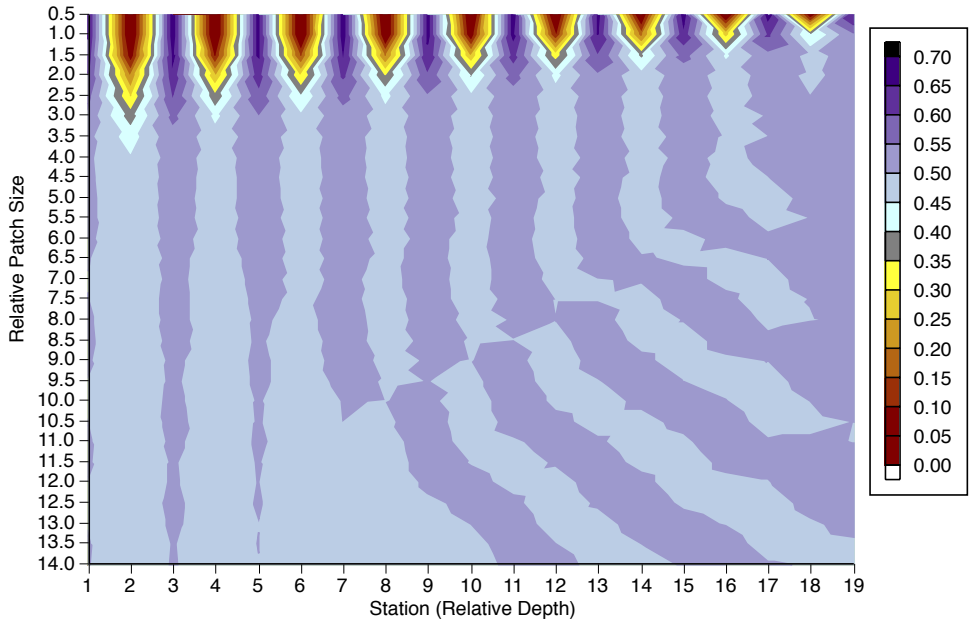

range 0.45 to 0.55. That is, this occurrence typically results in an overestimate of biomass or abundance when the adaptive stations are excluded. Conversely, a single mode at an adaptive station, or two modes, both on adaptive stations, routinely yield an underestimate of biomass or abundance; often extreme values of the ratio estimator are obtained. An example of a bimodal distribution with both modes at adaptive stations is shown for *Loligo* squid, January, 2004, on the Hudson Canyon transect (Figure 34). This transect yielded a ratio estimator of 0.399 (Table 16). A bimodal distribution in which one mode is adaptive and one fixed does not always yield an extreme value; however, when it does, these values are always produced by fixed-station-only underestimates of biomass or abundance. Such a distribution is exemplified by the distribution of silver hake, November, 2005, on the Baltimore Canyon transect (Figure 35). This transect yielded a ratio estimator of 0.439. Each of these results conform with the more theoretical treatments of Figures 26, and 28 through 33.

An unusual aspect of Tables 16 and 17 is the extreme values of the ratio estimators that occur when both modes of a bimodal distribution occur at fixed stations. Table 16 contains three examples, one for black sea bass and two for silver hake. Table 17 contains three examples, one for *Loligo* squid and two for silver hake. Focusing on Table 16, in one of three cases, the distribution of black sea bass in

Figure 30. Simulation of the Hudson Canyon transect using a depth-dependent gradient in swath area per station [equation (26)], a first-order or triangular-shaped patch [equation (28)], 10 fixed (odd number) and nine adaptive (even number) stations, all sampled, and a series of patch sizes. Patch size is defined relative to the swath area for station 2 (Figure 25). In this case, the simulation includes a bimodal patch dynamic in which one patch is centered on station 6, an adaptive station, and is of relative patch size 5. The other patch is varied in location and size according to the abscissa and ordinate values.

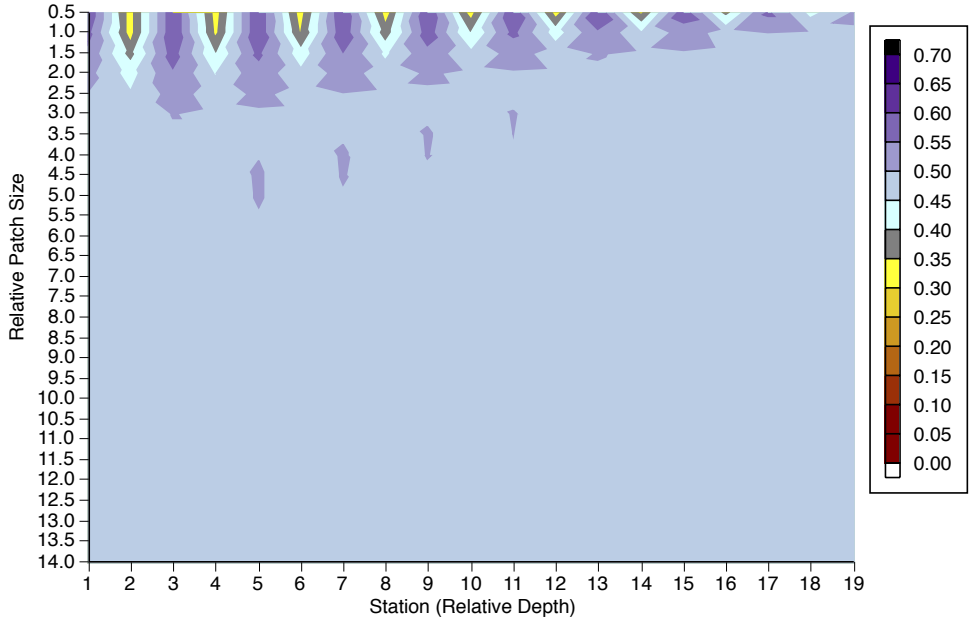

January, 2005, on the Hudson Canyon transect (Figure 36), the anticipated extreme overestimate, a ratio estimator value above 0.55, occurs. This transect yielded a ratio estimator of 0.575. But, in the other two cases, the converse is true. For silver hake, March and November, 2005, on the Hudson Canyon transect (Figures 24 and 37; Tables 16 and 17), both ratio estimators fall below 0.45. This counterintuitive outcome is obtained when one of the patches is relatively large and dome-shaped.

To simulate this condition, we adopt the true swath areas for each of the Hudson Canyon strata, rather than using equation (26), and simulate precisely the case of November, 2005 (Figure 24). Silver hake were distributed along the Hudson canyon transect in November, 2005, in two patches, a small one towards the upslope end of the transect and a larger one, containing about a factor of 10 more fish, towards the downslope end. Both modes fell on fixed stations. The results of this simulation are depicted in Figure 38. The patch is best described as a zero-order patch form (Figure 27). A rectangular patch, when the patch boundaries do not fall precisely on the stratum boundaries, will approximate a dome-shaped form, as is seen in the

Figure 31. Simulation of the Hudson Canyon transect using a depth-dependent gradient in swath area per station [equation (26)], a first-order or triangular-shaped patch [equation (28)], 10 fixed (odd number) and nine adaptive (even number) stations, all sampled, and a series of patch sizes. Patch size is defined relative to the swath area for station 2 (Figure 25). In this case, the simulation includes a bimodal patch dynamic in which one patch is centered on station 7, a fixed station, and is of relative patch size 5. The other patch is varied in location and size according to the abscissa and ordinate values.

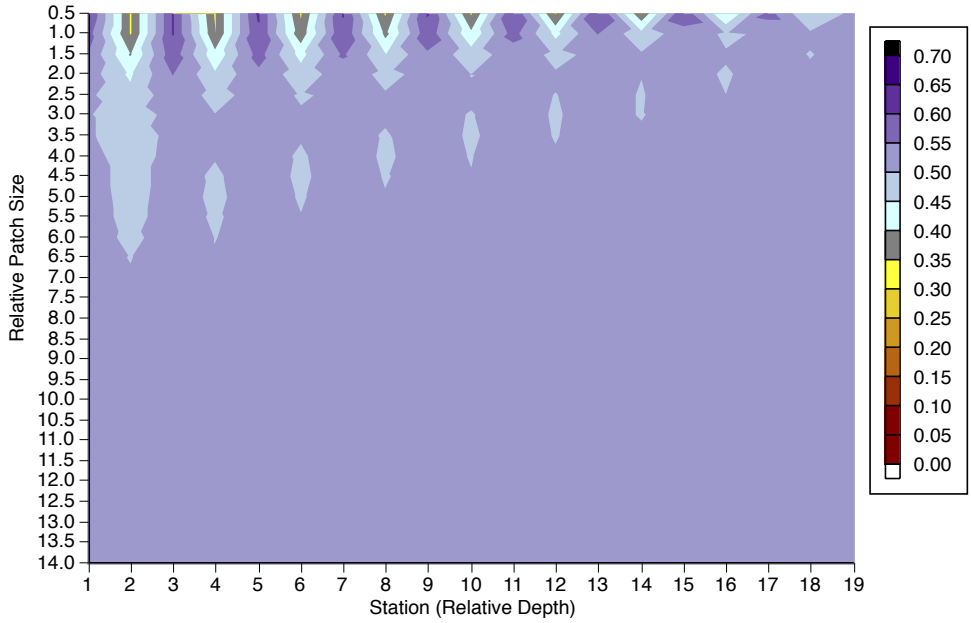

larger patch in Figure 24. The simulation shows that the larger patch dominates the biomass estimate and that reliance on the fixed stations only consistently produces a substantial underestimate of biomass regardless of the location and geographic extent of the smaller patch.

The fact that one patch contains a factor of 10 more fish than the other, however, is not the dominant effector of this outcome. Figure 39 shows the same simulation, except with both patches containing an equivalent quantity of fish. Excepting a few cases where one patch size is narrow and falls on a fixed station near the upslope boundary of the transect, this bimodal distribution consistently yields an underestimate of biomass when only the fixed stations are used. The degree of underestimate is lessened in comparison to Figure 38; that is, the frequency and extent to which this bimodal distribution generates an extreme underestimate is dependent upon the relative proportion of fish in the two patches. The fact that an underestimate is likely is dependent upon the presence of a dome-shaped patch centered on a fixed station.

Figure 32. Simulation of the Hudson Canyon transect using a depth-dependent gradient in swath area per station [equation (26)], a first-order or triangular-shaped patch [equation (28)], 10 fixed (odd number) and nine adaptive (even number) stations, all sampled, and a series of patch sizes. Patch size is defined relative to the swath area for station 2 (Figure 25). In this case, the simulation includes a bimodal patch dynamic in which one patch is centered on station 2, an adaptive station, and is of relative patch size 1. The other patch is varied in location and size according to the abscissa and ordinate values.

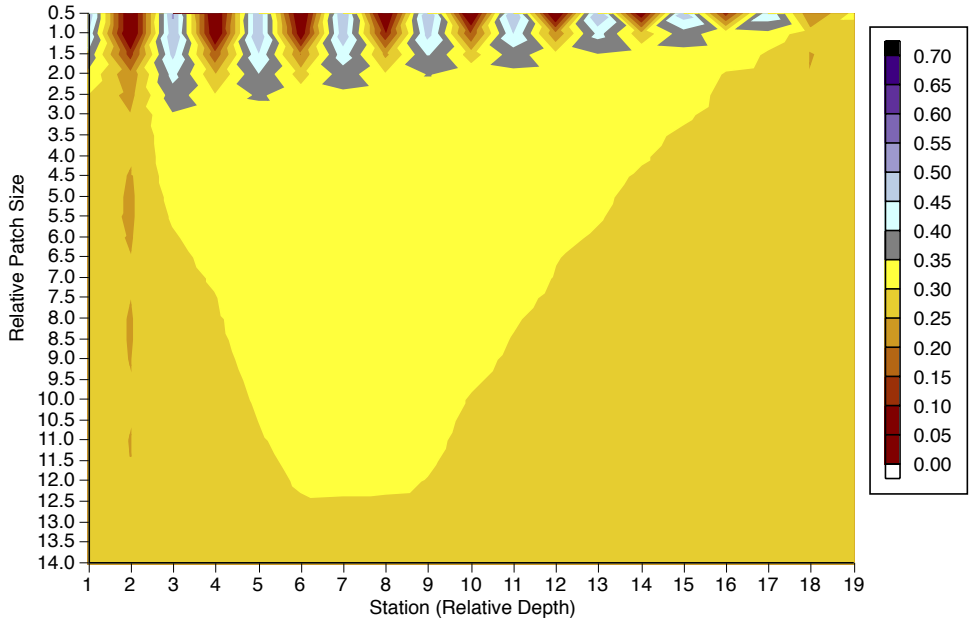

That the tendency towards underestimation is dependent on patch shape is shown by Figure 40. This simulation is identical to that shown in Figure 38, including the factor of ten difference in biomass between the two patches. However, the larger patch is simulated to be first-order in shape (Figure 27). That is, the concentration of fish declines more rapidly away from the center of the patch than in the simulation shown in Figure 38. In this case, the tendency towards underestimation is reversed. Nearly all cases show a degree of overestimation in biomass based on the fixed stations alone.

Now we know that cases where two bimodal patches occur on fixed stations that yield the counterintuitive underestimate of biomass based on the fixed stations alone are produced by a variant in patch shape in which the concentration of fish declines slowly from the center of the patch. Extreme values are obtained when this patch also contains a larger quantity of fish than the second patch. Patch form also can produce the same effect when the distribution is characterized by a single mode at a fixed station, as the case for *Loligo* squid on Hudson Canyon in January, 2005, shows (Table 17), but much more rarely. Only one such case exists in Tables

Figure 33. Simulation of the Hudson Canyon transect using a depth-dependent gradient in swath area per station [equation (26)], a first-order or triangular-shaped patch [equation (28)], 10 fixed (odd number) and nine adaptive (even number) stations, all sampled, and a series of patch sizes. Patch size is defined relative to the swath area for station 2 (Figure 25). In this case, the simulation includes a bimodal patch dynamic in which one patch is centered on station 6, an adaptive station, and is of relative patch size 1. The other patch is varied in location and size according to the abscissa and ordinate values.

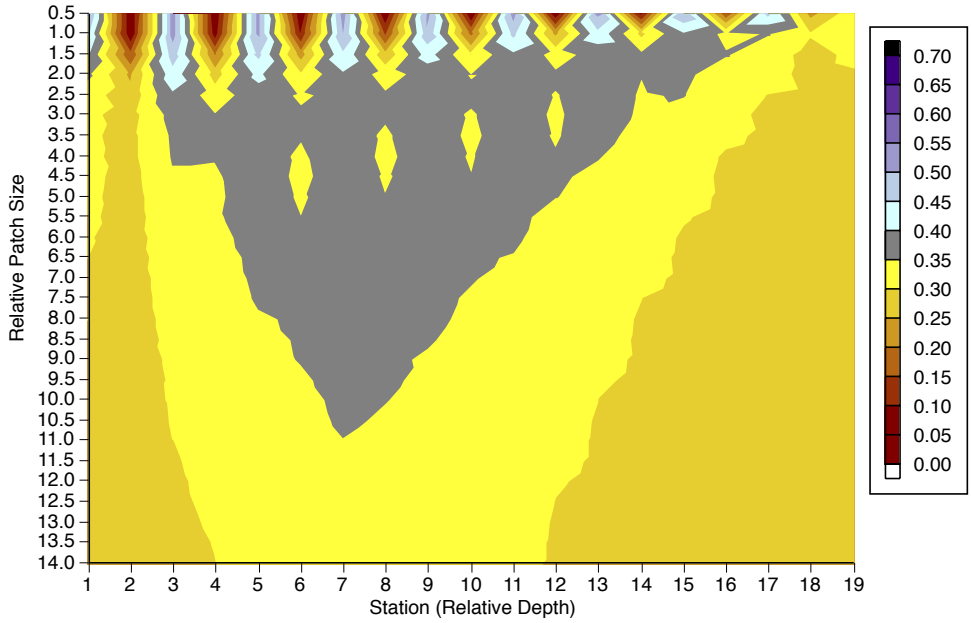

16 and 17 out of ten single-mode fixed-station cases therein identified.

The presence of underestimatees from distributions with fixed-station modes produced by patch forms of a kind described by a zero-order clustering process explains why underestimates, including extreme underestimates, are consistently more common than overestimates despite the likelihood of a mode falling on a fixed or adaptive station rarely diverging significantly from chance (Tables 14 and 15). Some cases where modes fall on fixed stations produce underestimates. The obverse case for adaptive stations never occurs. Modes on adaptive stations produce underestimates in essentially all cases.

Summary of Adaptive Sampling Protocol

The adaptive station protocol was introduced into the sampling program to provide a better description of the cross-shelf distribution of species. The protocol has proven to also provide data on the tendency of fish to be underestimated or overestimated given inadequate sampling density. Across all target species,

Table 16. Values of the biomass ratio estimator for black sea bass, *Loligo* squid, and silver hake estimated for each survey on the Hudson and Baltimore Canyon transects. For ratios < 0.45 and > 0.55, the modes were identified with A = single mode on an adaptive station, F = single mode on a fixed station, AA = a bimodal distribution with both modes on the adaptive stations, FF = a bimodal distribution with both modes on the fixed stations, and AF = a bimodal distribution in which one mode occurs on an adaptive station and the other on the fixed station.

	Black Sea Bass		*Loligo* Squid		Silver Hake	
	Ratio	Scenario	Ratio	Scenario	Ratio	Scenario
Hudson Canyon						
May-03	0.42918	A	0.57635	F	0.49476	
Jan-04	0.53759		0.39924	AA	0.37715	AF
Mar-04	0.49512		0.46907		0.49075	
May-04	0.51161		0.34408	AF	0.48813	
Nov-04	0.51419		0.38724	AF	0.38491	AA
Jan-05	0.57508	FF	0.47760		0.47702	
Mar-05	0.54349		0.53540		0.44316	FF
May-05	0.52393		0.45034		0.49119	
Nov-05	0.50000		0.49164		0.42047	FF
Baltimore Canyon						
May-03	0.16399	A	0.58861	F	0.30737	A
Mar-04	0.48201		0.47616		0.46842	
Nov-04	0.50000		0.48837		0.38648	A
Jan-05	0.44024	A	0.48285		0.40704	A
Mar-05	0.38887	AF	0.41505	AF	0.54068	
May-05	0.48902		0.55921	F	0.45989	
Nov-05	0.57781	F	0.28044	AF	0.43986	AF

on the average, the bias is towards underestimation. Some, such as silver hake, are consistently biased in this way. Extreme overestimates or underestimates also occur commonly, and are biased. Extreme underestimates occur more frequently. Modeling of the transect design shows that those cases where the fixed stations alone provide data clearly inadequate for the estimate of abundance or biomass occur when sampling density is inadequate to identify the center of the patch or to identify the shape of the patch. This dynamic occurs, even though the fixed station sampling density included 10 stations from 40 to 250 fm, a relatively dense sampling in comparison to the federal multispecies surveys in this region of the continental shelf (Table 8). An opportunity exists to utilize information of this kind to evaluate the adequacy of sample density in re-designing survey efforts for the NMFS strata covering the outer half of the continental shelf and to obtain correction factors for given sample densities when adequate sample density cannot be achieved due to logistical constraints.

Table 17. Values of the ratio estimator for numerical abundance for black sea bass, *Loligo* squid, and silver hake estimated for each survey on the Hudson and Baltimore Canyon transects. For ratios < 0.45 and > 0.55, the modes were identified with A = single mode on an adaptive station, F = single mode on a fixed station, AA = a bimodal distribution with both modes on the adaptive stations, FF = a bimodal distribution with both modes on the fixed stations, and AF = a bimodal distribution in which one mode occurs on an adaptive station and the other on the fixed station.

	Black Sea Bass		*Loligo* Squid		Silver Hake	
	Ratio	Scenario	Ratio	Scenario	Ratio	Scenario
Hudson Canyon						
May-03	0.48159		0.55721	FF	0.48094	
Jan-04	0.54122		0.26672	AF	0.23713	AF
Mar-04	0.55039	F	0.54753		0.47266	
May-04	0.50996		0.31378	AF	0.49509	
Nov-04	0.57797	F	0.46165		0.38960	AA
Jan-05	0.53348		0.43499	F	0.50676	
Mar-05	0.53034		0.50435		0.37162	AA
May-05	0.35682	AF	0.47762		0.50582	
Nov-05	0.50000		0.49221		0.38322	FF
Baltimore Canyon						
May-03	0.15233	A	0.56519	F	0.31492	A
Mar-04	0.47624		0.51985		0.45702	
Nov-04	0.50000		0.51491		0.34119	A
Jan-05	0.36893	A	0.45333		0.32281	A
Mar-05	0.11911	AA	0.48148		0.64279	FF
May-05	0.49734		0.59890	F	0.48193	
Nov-05	0.58345	F	0.13680	AF	0.49755	

Literature Cited

Battista, T.D. 2003. Resampling methods for estimating dispersion indices in random and adaptive designs. *Environ. Ecol. Stat.* 10:83-93.

Bunt, J.S., W.T. Williams and H.J. Clay. 1984. Detection of species sequences across environmental gradients. *Mar. Ecol. Prog. Ser.* 24:197-199.

Clark, P.J. and F.C. Evans. 1954. Distance to nearest neighbor as a measure of spatial relationships in populations. *Ecology* 35:445-453.

Conover, W.J. 1980. *Practical nonparametric statistics.* New York: John Wiley & Sons. 493 pp.

Davis, J.C. 1986. *Statistics and data analysis in geology.* New York: John Wiley &

Figure 34. Swath-area biomass for *Loligo* squid along the Hudson Canyon transect in January, 2004. Tow numbers indicate the sampling sequence during the cruise. Tows are ordered shallowest to deepest along the abscissa according to the depth profile shown as the solid line.

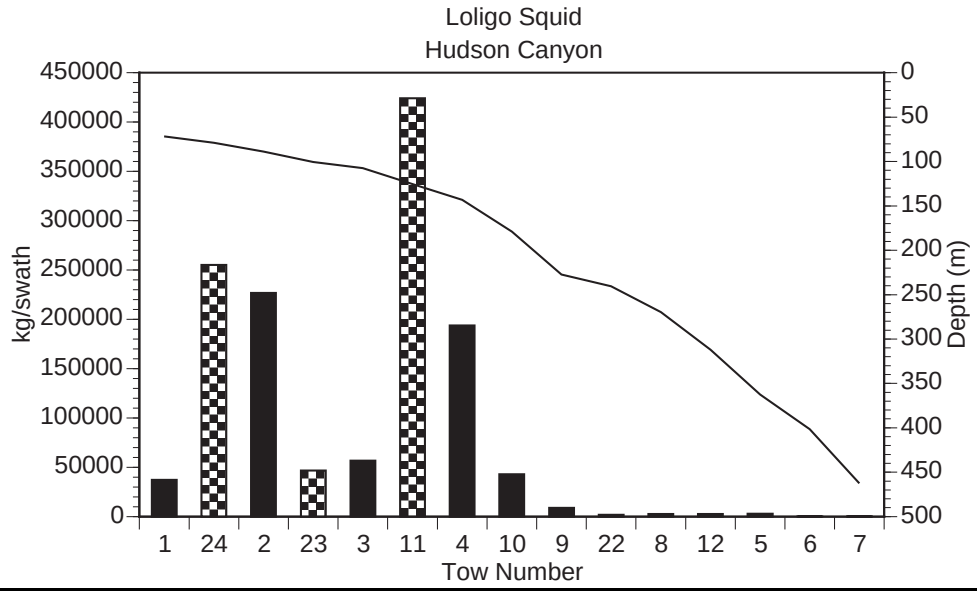

Figure 35. Swath-area biomass for silver hake along the Baltimore Canyon transect in November, 2005. Tow numbers indicate the sampling sequence during the cruise. Tows are ordered shallowest to deepest along the abscissa according to the depth profile shown as the solid line.

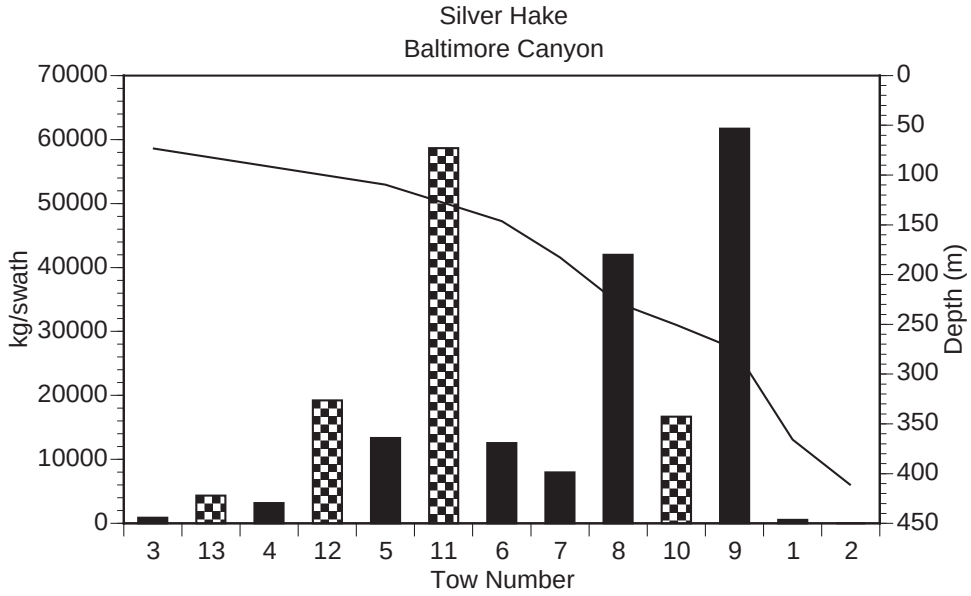

Sons. 646 pp.

Figure 36. Swath-area biomass for black sea bass along the Hudson Canyon transect in January, 2005. Tow numbers indicate the sampling sequence during the cruise. Tows are ordered shallowest to deepest along the abscissa according to the depth profile shown as the solid line.

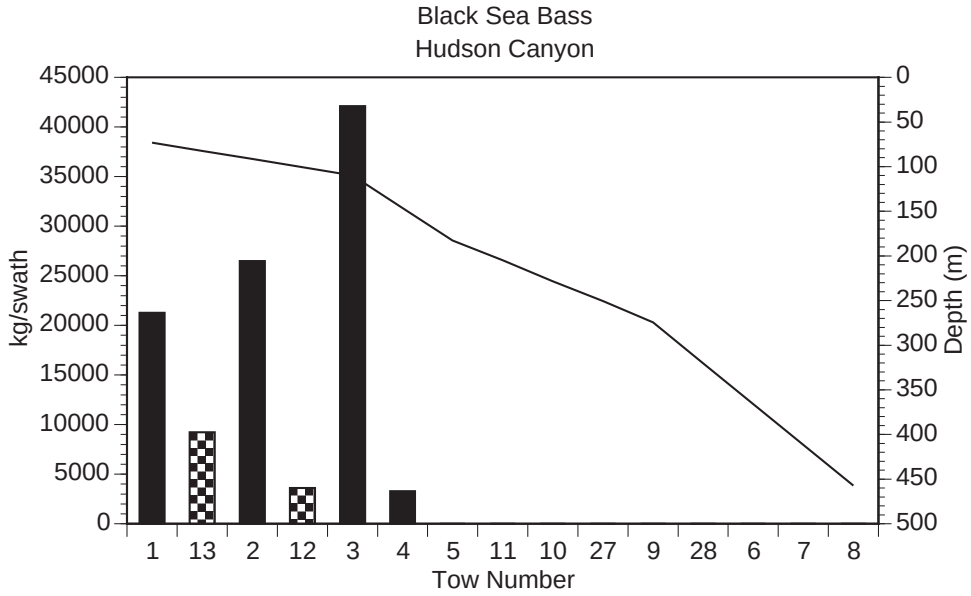

Figure 37. Swath-area biomass for silver hake along the Hudson Canyon transect in March, 2005. Tow numbers indicate the sampling sequence during the cruise. Tows are ordered shallowest to deepest along the abscissa according to the depth profile shown as the solid line.

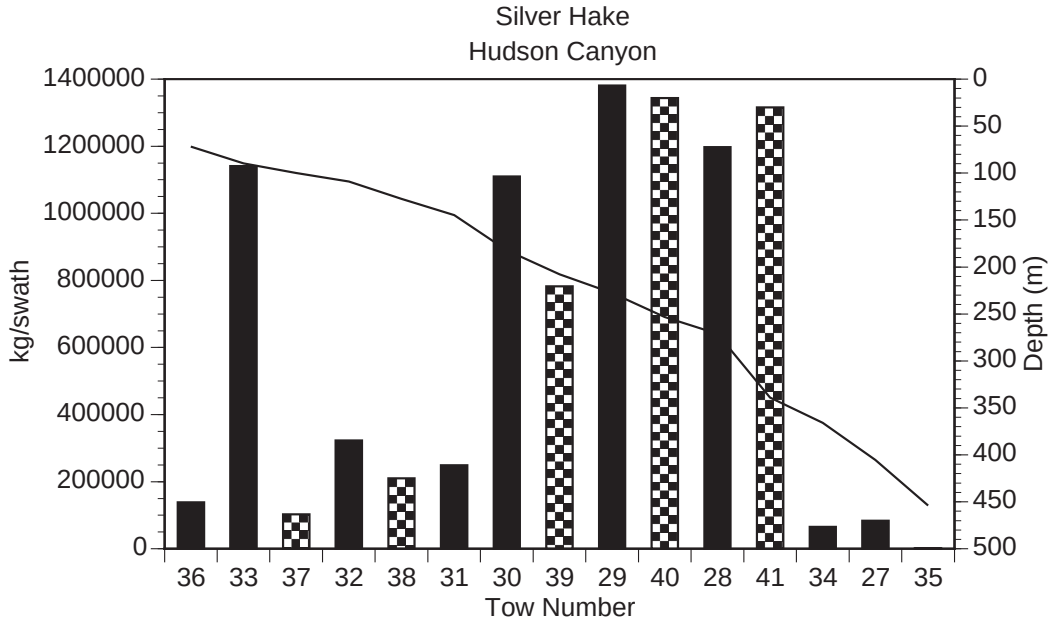

Figure 38. Simulation of the Hudson Canyon transect for November, 2005, for silver hake using an exact rendition of the depth-dependent gradient in swath area per station (Figure 25), a zero-order or rectangular-shaped patch [equation (27)] defined in size to simulate a dome-shaped patch as sampled, 10 fixed (odd number) and nine adaptive (even number) stations, all sampled, and a series of patch sizes. Patch size is defined relative to the swath area for station 2 (Figure 25). In this case, the simulation includes a bimodal patch dynamic in which one patch is centered on station 11, an adaptive station, contains 200,000 kg of silver hake, and is of relative patch size 0.5. The other patch contains 20,000 kg and is varied in location and size according to the abscissa and ordinate values. In the case of the sampled distribution shown in Figure 24, this patch was in reality at station 5 and had a relative patch size of 1.0.

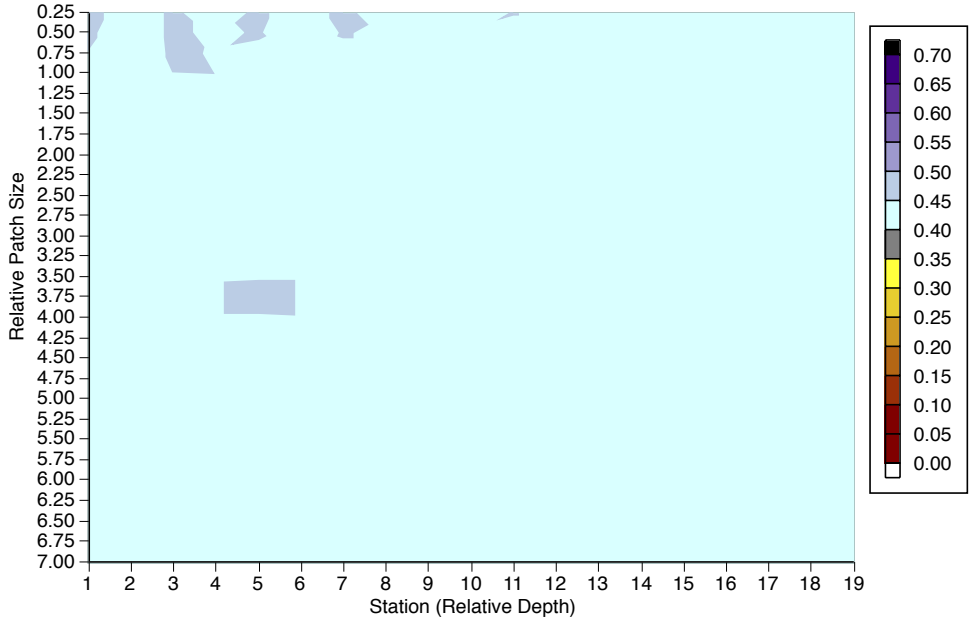

Elliott, J.M. 1977. Some methods for the statistical analysis of samples of benthic invertebrates. *Freshwater Biological Association Sci. Publ.* 25:1-157.

Farris, R.A. and E.W. Lindgren. 1984. *A posteriori* investigation of spatial arrangements in Gnathostomulida and Copepoda. *Int. Rev. ges. Hydrobiol.* 69:443-450.

Findlay, S.E.G. 1982. Influence of sampling scale on apparent distribution of meiofauna on a sandflat. *Estuaries* 5:322-324.

Folmer, O. and M. Pennington. 2000. A statistical evaluation of the design and precision of the shrimp trawl survey off West Greenland. *Fish. Res.* 49:165-178.

Green, R.H. 1989. Power analysis and practical strategies for environmental

Figure 39. Simulation of the Hudson Canyon transect for November, 2005, for silver hake using an exact rendition of the depth-dependent gradient in swath area per station (Figure 25), a zero-order or rectangular-shaped patch [equation (27)] defined in size to simulate a dome-shaped patch as sampled, 10 fixed (odd number) and nine adaptive (even number) stations, all sampled, and a series of patch sizes. Patch size is defined relative to the swath area for station 2 (Figure 25). In this case, the simulation includes a bimodal patch dynamic in which one patch is centered on station 11, an adaptive station, contains 200,000 kg of silver hake, and is of relative patch size 0.5. The other patch contains an equivalent quantity of fish and is varied in location and size according to the abscissa and ordinate values.

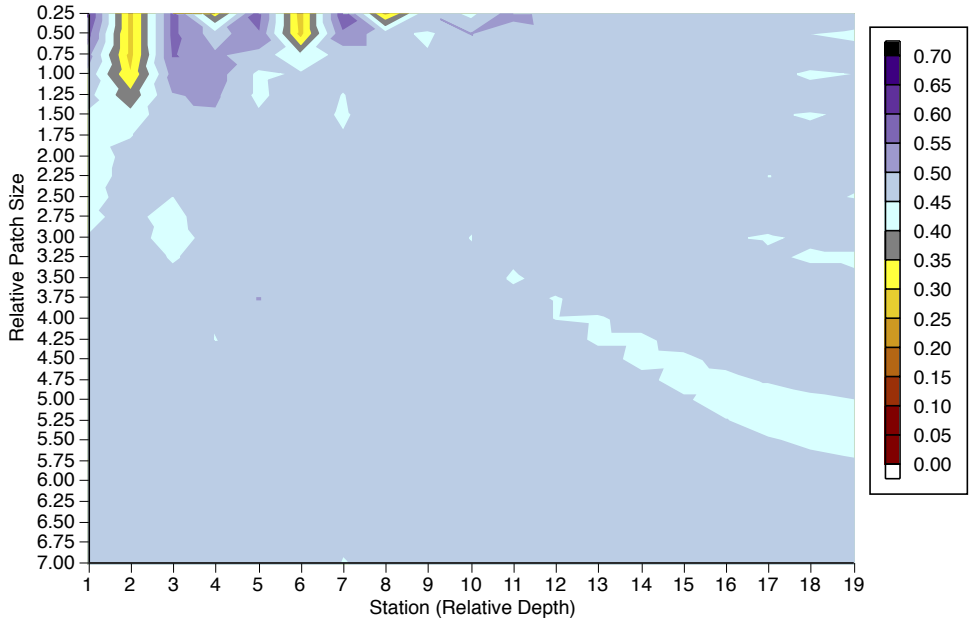

monitoring. *Environ. Res.* 50:195-205.

Green, R.H. and R.C. Young. 1993. Sampling to detect rare species. *Ecol Appl* 3:351-366.

Hjellvik, V., O.R. Godø, D. Tjøstheim. 2002. The measurement error in marine survey catches: The bottom trawl case. *Fish. Bull.* 100:720-726.

Jensen, A.C. 1965. Life history of the spiny dogfish. *Fish. Bull.* 65:527:554.

Johnsen, E. 2003. Improving the precision of length frequency distribution estimates from trawl surveys by including spatial covariance – using Namibian *Merluccius capensis* as an example. *Fish. Res.* 62:7-20.

Jumars, P.A., D. Thistle and M.L. Jones. 1977. Detecting two-dimensional spatial

Figure 40. Simulation of the Hudson Canyon transect for November, 2005, for silver hake using an exact rendition of the depth-dependent gradient in swath area per station (Figure 25), a first-order or triangular-shaped patch [equation (27)], 10 fixed (odd number) and nine adaptive (even number) stations, all sampled, and a series of patch sizes. Patch size is defined relative to the swath area for station 2 (Figure 25). In this case, the simulation includes a bimodal patch dynamic in which one patch is centered on station 11, an adaptive station, contains 200,000 kg of silver hake, and is of relative patch size 0.5. The other patch contains a 20,000 kg of fish and is varied in location and size according to the abscissa and ordinate values.

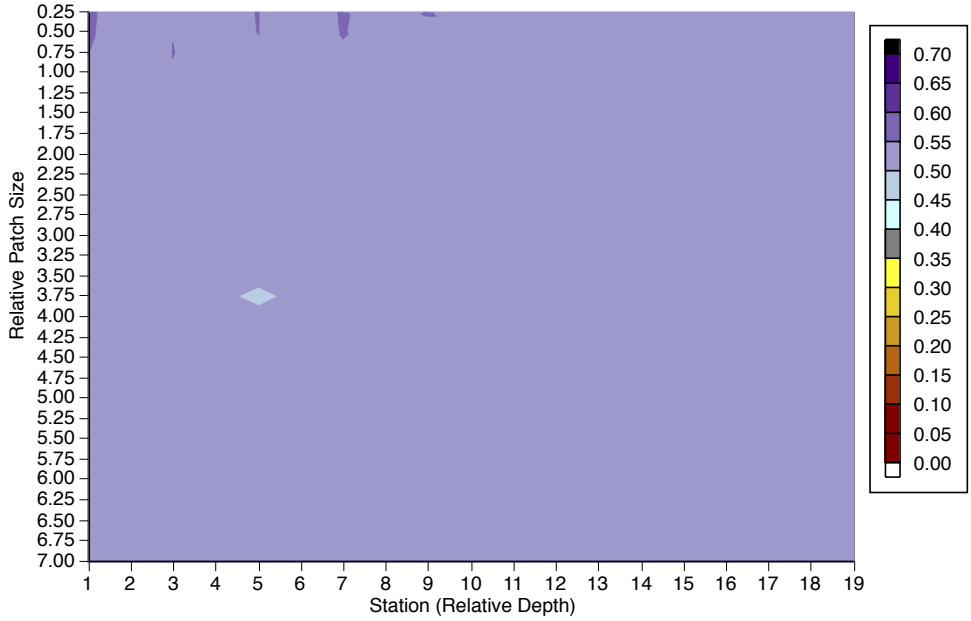

structures in biological data. *Oecologia (Berl.)* 28:109-123.

McCullagh, M.J. and C.G. Ross. 1980. Delaunay triangulation of a random dataset for isarithmic mapping. *Cartography J.* 17:93-99.

Meyers M.B., E.N. Powell, and H. Fossing. 1988. Movement of oxybiotic and thiobiotic meiofauna in response to changes in pore-water oxygen and sulfide gradients around macro-infaunal tubes. *Mar. Biol. (Berl.)* 98:395-414.

Murawski, S.A. 1993. Climate change and marine fish distributions: Forecasting from historical analogy. *Trans. Am. Fish. Soc.* 122:647-658.

NEFSC. 1998. 27th Northeast Regional stock assessment workshop (27th SAW): Stock assessment review committee (SARC) consensus summary of assessments. *NEFSC Ref. Doc.* 98-07, 360 pp.

NEFSC. 1999. 29^{th} Northeast Regional stock assessment workshop (29^{th} SAW): Stock assessment review committee (SARC) consensus summary of assessments. *NEFSC Ref. Doc.* 99-14, 347 pp.

NEFSC. 2002. 34^{th} Northeast Regional stock assessment workshop (34^{th} SAW): Stock assessment review committee (SARC) consensus summary of assessments. *NEFSC Ref. Doc.* 02-06, 346 pp.

NEFSC. 2006. 42^{nd} Northeast Regional Stock Assessment Workshop (42^{nd} SAW) Stock Assessment Report. Part A: Silver Hake, Atlantic Mackerel, & Northern Shortfin Squid. Part B: Expanded Multispecies Virtual Population Analysis (MSVPA-X) Stock Assessment Model. *NEFSC Ref. Doc.* 06-09, pp. 308.

NOAA. 1999. Essential fish habitat source document: spiny dogfish, *Squalus acanthis*, life history, and habitat characteristics. *NOAA Tech. Mem.* NMFS-NE-150.

NRDC. 2001. *Priority ocean areas for protection in the Mid-Atlantic.* Natural Resources Defense Council, 59 pp.

Pennington, M. and J.H. Vølstad. 1991. Optimum size of sampling unit for estimating the density of marine populations. *Biometrics.* 47:717-723.

Peterson, C.H., L.L. McDonald, R.H. Green and W.P. Erickson. 2001. Sampling design begets conclusions: The statistical basis for detection of injury to and recovery of shoreline communities after the 'Exxon Valdez' oil spill. *Mar. Ecol. Prog. Ser.* 210:255-283.

Petitgas, P and T. LaFont. 1997. EVA2: Estimation variance version 2: A geostatistical software on *Windows 95* for the precision of fish stock assessment surveys. *ICES* CM 1997/Y:22, 22 pp.

Powell, E.N., A.J. Bonner, S.E. King and E.A. Bochenek. in press. Survey augmentation using commercial vessels in the Mid-Atlantic Bight: Sampling density and relative catchability. *J. Appl. Ichthyol.*

Powell, E.N., A.J. Bonner, B. Muller, and E.A. Bochenek. 2004. Assessment of the effectiveness of scup bycatch-reduction regulations in the *Loligo* squid fishery. *J. Environ. Manag.* 71:155-167.

Powell, E.N., J. Song, M.S. Ellis and E.A. Wilson-Ormond. 1995. The status and long-term trends of oyster reefs in Galveston Bay, Texas. *J. Shellfish Res.* 14:439-457.

Powell, E.N., M.E. White, E.A. Wilson and S.M. Ray. 1987. Small-scale spatial distribution of a pyramidellid snail ectoparasitic, *Boonea impressa*, in relation to its host, *Crassostrea virginica*, on oyster reefs. *P.S.Z.N.I.: Mar. Ecol.* 8:107-130.

Shepherd, G.R., and M. Terceiro. 1994. The summer flounder, scup, and black sea bass fishery of the Middle Atlantic Bight and southern New England. *NOAA Tech. Rpt.* NMFS 122, 13 pp.

Smith, D.R., R.E. Villella and D.P. Lemarie. 2003. Application of adaptive cluster sampling to low-density populations of freshwater mussels. *Environ. Ecol. Stat.* 10:7-15.

Underwood, A.J. 1978. The detection of non-random patterns of distribution of species along a gradient. *Oecologia (Berl.)* 36:317-326

Vignaux, M. 1996. Analysis of spatial structure in fish distribution using commercial catch and effort data from the new Zealand hoki fishery. *Can. J. Fish. Aquat. Sci.* 53:963-973.

Wallace, J.R. and C.W. West. 2006. Measurements of distance fished during the trawl retrieval period. *Fish. Res.* 77:285-292.

Witman, J.D., R.J. Etter and F. Smith. 2004. The relationship between regional and local species diversity in marine benthic communities: A global perspective. *Proc. Natl. Acad. Sci.* 101:15664-15669.